Copyright Warning & Restrictions

The copyright law of the United States (Title 17, United States Code) governs the making of photocopies or other reproductions of copyrighted material.

Under certain conditions specified in the law, libraries and archives are authorized to furnish a photocopy or other reproduction. One of these specified conditions is that the photocopy or reproduction is not to be "used for any purpose other than private study, scholarship, or research." If a, user makes a request for, or later uses, a photocopy or reproduction for purposes in excess of "fair use" that user may be liable for copyright infringement,

This institution reserves the right to refuse to accept a copying order if, in its judgment, fulfillment of the order would involve violation of copyright law.

Please Note: The author retains the copyright while the New Jersey Institute of Technology reserves the right to distribute this thesis or dissertation

Printing note: If you do not wish to print this page, then select "Pages from: first page # to: last page #" on the print dialog screen

ABSTRACT

ADVANCED CHARACTERIZATION AND LEACHING BEHAVIOR OF HEXAVALENT AND TRIVALENT CHROMIUM FROM WASTE MATERIAL

by
Erik Moerman

In this thesis we employed advanced characterization techniques such as XRF, XRD, XPS, SEM, and EDS to provide detailed information about the chromium waste _ specifically chromium valence states (Cr(VI) and Cr(III)), and their chemical association with other phases in the waste matrix.

The removal of Cr(VI) was accomplished by leaching with aqueous solutions containing inorganic anions such as Cl^-, SO_4^{2-}, PO_4^{3-}, and others. Cr(VI) can be released from the waste by a combination of desorption and ion exchange processes. The efficiency and kinetics of displacing CrO_4^{2-} from the waste by anions was extensively studied.

Cr(III) removal was achieved by the oxidative dissolution process - i.e., by using different oxidants at various pH conditions. We defined the mechanisms for Cr(III) transformation to Cr(VI) and the leaching of the latter into the environment under different pH conditions. We assessed the conditions and rate for such conversion and leaching processes.

ADVANCED CHARACTERIZATION AND LEACHING BEHAVIOR OF HEXAVALENT AND TRIVALENT CHROMIUM FROM WASTE MATERIAL

by
Erik Moerman

A Thesis
Submitted to the Faculty of
New Jersey Institute of Technology
in Partial Fulfillment of the Requirements for the Degree of
Master of Science in Environmental Engineering

Department of Civil and Environmental Engineering

May 1996

APPROVAL PAGE

ADVANCED CHARACTERIZATION AND LEACHING BEHAVIOR OF HEXAVALENT AND TRIVALENT CHROMIUM FROM WASTE MATERIAL

Erik Moerman

Dr. Mohamed E. Labib, Thesis Advisor — Date
Research Professor of Civil and Environmental Engineering, NJIT

Dr. William R. Spillers, Committee Member — Date
Professor of Civil and Environmental Engineering and Chairman
of the Department of Civil and Environmental Engineering, NJIT

Dr. Dorairaja Raghu, Committee Member — Date
Professor of Civil and Environmental Engineering, NJIT

BIOGRAPHICAL SKETCH

Author: Erik Moerman

Degree: Master of Science in Environmental Engineering

Date: May 1996

Undergraduate and Graduate Education:

- Master of Science in Environmental Engineering,
  New Jersey Institute of Technology, Newark, New Jersey, 1996

- Civil Engineer Chemistry,
  Free University of Brussels, Brussels, Belgium, 1994

Presentations and Publications:

Moerman, Erik, July 1994. "Catalysis by means of a FEPC-y Zeolite." *VUB Press*, Brussels, Belgium. Thesis.

This thesis is dedicated to
my parents.

ACKNOWLEDGMENT

The author wishes to express his sincere gratitude to his supervisor, Dr. Mohamed E. Labib, for his guidance, friendship, and moral support throughout this research.

The author is grateful to Professor William Spillers and Professor Dorairaja Raghu for serving as members of the committee.

TABLE OF CONTENTS

TABLE OF CONTENTS
(Continued)

Chapter **Page**

TABLE OF CONTENTS
(Continued)

Chapter **Page**

TABLE OF CONTENTS
(Continued)

LIST OF TABLES

LIST OF TABLES
(Continued)

Table **Page**

LIST OF FIGURES

LIST OF FIGURES
(Continued)

Figure **Page**

LIST OF FIGURES
(Continued)

Figure **Page**

CHAPTER 1

INTRODUCTION

1.1 Heavy Metal Contamination and Effect on Public Health

Modern industrial activities have resulted in heavy metal contamination of various environmental media, including water, soil and air. The disposal practices that took place before the advent of recent strict environmental regulations account for the majority of existing heavy metal contamination in the world. Heavy metal contamination includes industrial waste waters and liquids, solid residues of industrial processes and volatile compounds containing heavy metal ions, as in the case of lead emission from automobiles. The common heavy metals are copper, silver, zinc, cadmium, mercury, lead, chromium, selenium, arsenic, and nickel. High levels of heavy metals in drinking water, soils, plants, food and air constitute danger to public health. The participation of these metals is essential for the survival of organic life, including humans. However, heavy metals are only needed in trace amounts. In cases where the concentration of heavy metals exceeds the levels necessary for normal nutritional response (or exposure), the metals become toxic or even lethal. The toxicity of a metal is influenced by the metal's accessibility, mobility, bioavailability and appearance in the environment. Heavy metal 's toxicological tolerance levels for mammal and man are listed in Table 1.1.

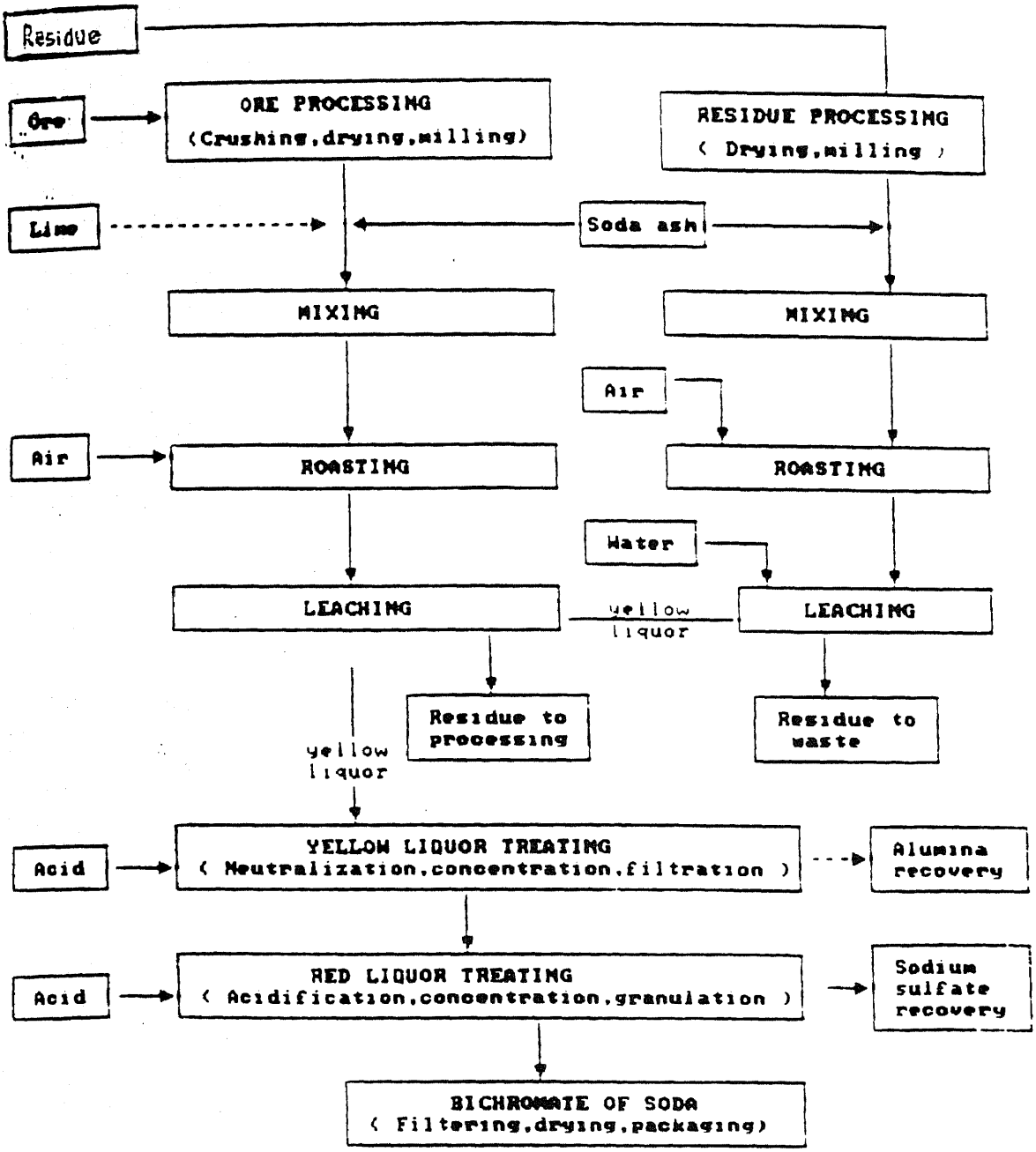

Figure 1.1 Flow chart of chromium production (Ref. 9).

Table 1.1 Toxicological tolerance levels of some metals (Ref. 2).

Element	Compound	Mammal	Man
Al	$Al(SO_4)_3$	12 g/kg	
Ag	Ag-compound		0.05 mg/l chronic *
As	As-compound	2-15 mg/kg	0.05 mg/l chronic *
Ba	$BaCl_2$	30-500 mg/kg	3.3-8.3 mg/kg
B	H_3BO_3	1-5.1 g/kg	5-20 g
Cd	$CdCl_2$	0.07-0.15 mg/kg	50-500 mg/kg
Co	Co-compound	0.7-1.5 g/kg	50-500 mg/kg
Cr	Chromate	0.5-11 mg/l chronic *	0.5-5 g/kg
Cr	$Cr_2(SO_4)_3$		
Cu	$CuSO_4$	8 g	8 g
Fe	$FeSO_4$	0.5-5 g/kg	0.5-5 g/kg
Hg	$HgCl_2$	0.1-1 g	
Mn	Mn-compounds		0.5-5 g/kg
Ni	Ni-compounds		50-500 mg/kg
Pb	$Pb(NO_3)_2$	2 g/kg	
Se	Se-compounds	5-10 mg/l chronic *	0.01 mg/l chronic *
Zn	$ZnSO_4$	1.9-2.2 mg/kg	

(*) Chronic effects are long-term toxic effects such as cancer.

In this thesis we are specially concerned with chromium contamination which is considered as one of the most potent toxics of all heavy metals. We are specifically targeting the chromium residue fill problem of Hudson County, New Jersey, and other equivalent sites worldwide. The main objectives of this research work are to apply advanced characterization techniques to understand the nature of the chromium in residue-fill materials, and to develop treatment processes for this type of industrial waste. One of the major issues that we address in this work deals with how the two valence states of chromium (Cr(III) and Cr(VI)) behave in the environment and how can we consider them in treatment processes.

1.2 Origin of the Chromium Residue Fill Waste

The waste in the landfill of interest to this research is a residue of chromium ore processing plants. Between 1905 and 1976, chromium processing plants operated in Hudson County, New Jersey, and are responsible for existing chromium waste sites.

In chromium refining processes, soluble chromates and dichromates were produced from chromite ore. Chromite ore [(Fe, Mg)O.(Cr, Fe, $Al)_2O_3$] contains 45 to 50 % Cr_2O_3. A flow chart of this manufacturing process is given in Figure 1.1 (Ref. 9). In this refining process, the chromite ore was mixed with lime (or other basic solids) and heated in air to 1300-1500 ^{0} C. In this step, Cr(III) was converted to soluble chromates or dichromates - by oxidative dissolution. The material generated from the oxidation step was used to extract soluble Cr(VI) species _ the product of the refining operation. The residue of this process was disposed of as the fill material in sites located in Hudson County. The solid residue that was produced contained between 1 and 7 % chromium (Ref. 7), depending on the efficiency of the oxidation and extraction steps. These residues have resulted in a major chromium contamination in New Jersey. According to NJ-DEP, this is possibly the major environmental problem in New Jersey.

1.3 Chemistry of Chromium in the Aquatic Environment

In the natural environment, chromium exists in two stable oxidation states: Cr(VI) and Cr(III). The ratio of the two valence states is affected by the oxidation potential and pH of the aquatic environment, including water and solids in the soil. In general, at oxidizing conditions the hexavalent form will predominate, while under reducing conditions the trivalent form will predominate. The hexavalent form can exist as chromate or dichromate, depending on the pH, concentration and oxidation potential. In the waste, we only have to consider chromate as the major Cr(VI) specie. Chromate can exist as $HCrO_4^-$ and CrO_4^{2-}, depending on the pH. $HCrO_4^-$ is the dominant specie at low pH and CrO_4^{2-} is dominant at high pH. On the other hand, Cr(III) may exist in different forms depending on the pH. At acidic conditions Cr(III) will be a stable cation. By increasing the pH, dissolved species of Cr(III) will form: $Cr(OH)_2^+$, $Cr(OH)_3^0$, and $Cr(OH)_4^-$, respectively. The various chromium species and their domains of existence are given in Figure 1.2 (Ref. 6).

Cr(III) and Cr(VI) species differ greatly in their solubility in aqueous solutions. Cr(VI) is highly soluble under all circumstances. Cr(III), on the other hand, exists as solid phases (Cr_2O_3 and $Cr(OH)_3$) that have low solubility. The above solubility behavior indicates that Cr(VI) is easily transported in the environment and that the mobility of Cr(III) is limited due to its low solubility characteristics.

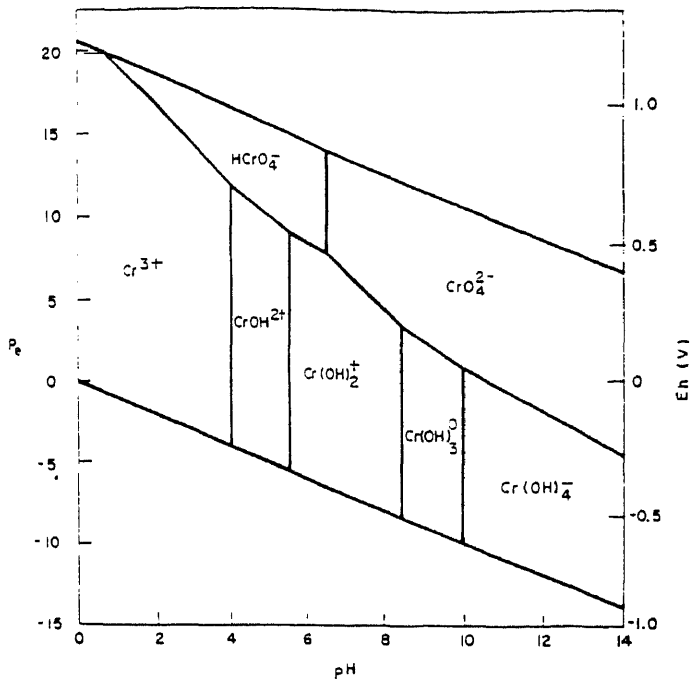

Figure 1.2 Areas of dominance of dissolved chromium species at equilibrium in the system Cr + H_2O + O_2 at 25 ^{0}C and 1 atm (Ref. 6).

We must be concerned, however, with the possibility of conditions that may transform Cr(III) to Cr(VI) in the environment. This is one of the objectives of this research.

1.4 Toxicity of Chromium

As discussed earlier, Cr(III) is rather immobile in the aqueous environment. Toxicological studies indicate that Cr(III) is a relatively inactive genotoxic agent. Cr(VI), on the other hand, can be easily transported in the aqueous environment and has the ability to cross the cell membranes. Cr(VI) is considered to be toxic to humans, animals and plants. Since Cr(III) can transform into the toxic Cr(VI)

under oxidizing conditions, such conversion needs to be understood and controlled. Two major toxic effects of Cr(VI) are now known:

(a) Acute response: This is mostly confined to the effect of Cr(VI) as an agent for "contact dermatitis", and

(b) Chronic response: The chronic response of Cr(VI) is mostly confined to inhaled particles. It has been clinically proven that Cr(VI) can cause lung cancer in humans.

1.5 Characterization Techniques

1.5.1 Conventional versus Advanced Characterization

Heavy metal contaminated soil or waste is conventionally characterized by particle size distribution, organic matter content, soil pH in water suspensions, major elemental analysis and metal concentration. The above properties are determined by wet chemical digestion, followed by analytical techniques using atomic absorption, mass-spectroscopy, ICPMS, etc. The analyses are cheap and simple, but the information generated is non specific and often incomplete. Digestion steps in conventional wet techniques may influence the original structure of the sample, which may result in inaccurate conclusions about the soil or waste under consideration. An excellent example can be demonstrated by considering the case of chromium-containing waste. Since chromium primarily exists in two forms, Cr(III) and Cr(VI), both species may be present together in the same material. Cr(VI) is normally analyzed by colorimetric methods (EPA

Method 3060A). Cr(III) is always determined from the difference between total Cr and Cr(VI) concentrations. In order to perform the colorimetric method, the sample must be digested for 60 minutes at a temperature of 90-95 ^{0} C in a solution containing 0.28M Na_2CO_3 / 0.5M NaOH. During this digestion step, reducing agents such as Fe(II) and organic matter (or others) may be released in the solution. This will cause a shift of the original Cr(VI)/ Cr(III) ratio towards more Cr(III). The opposite is true; if the sample has oxidizing species, the Cr(VI) concentration will appear higher than its actual concentration. To prevent this confusion, more advanced techniques that do not destroy sample structure or interfere with the analysis are needed. This may be done by applying advanced characterization techniques in the solid state without the need for chemical digestion. We used XPS for this purpose.

Furthermore, conventional characterization techniques do not provide sufficient information about the chemical environment of the heavy metal and its association with the matrix components (or phases) of the host waste or soil. It is extremely important to acquire sufficient knowledge about where and how the heavy metal is present in the waste. The ability to obtain such information would provide us with a better idea about how the heavy metal can be released or leached into the environment or during human exposure. Equally important, such detailed knowledge leads to the development of more efficient treatment technologies. For the above reasons, we have targeted the development of

advanced characterization techniques for use with waste and earth materials like soils.

1.5.2 Elements of Advanced Characterization

Recent advances in physics and material science have resulted in the development of several advanced characterization techniques. Such advanced techniques can be applied to obtain detailed information about the heavy metal, its chemical environment, and physical distribution within the waste matrix. Such detailed information could not be provided by the conventional techniques described above. Most advanced characterization techniques are based on using the material in the solid state without the need for chemical digestion or dissolution. Table 1.2 presents some advanced techniques, their basis and information generated by applying them.

1.5.3 Principles of Each of the Techniques

1.5.3.1 X-ray Fluorescence (XRF) X-ray fluorescence spectrometry is a nondestructive instrumental method for qualitative and quantitative analysis of chemical elements in solids. XRF is a technique based on the wave lengths and intensities of x-ray-excited spectral lines emitted from the elements in the solid sample. In XRF, primary x-rays (usually from an x-ray tube) excite each element in the sample to emit x-ray spectral lines. The wavelengths of the spectral lines

are characteristic of each element (qualitative analysis) while their intensities are related to concentration of the element (quantitative analysis) in the sample.

Any analytical method involving x-ray spectral lines must provide a means to permit a resolved line of each element to be measured without interference with others. In the case of XRF, the wavelength dispersion technique is used. The x-rays emitted by the sample are separated spacially (by wavelength) using crystal diffraction prior to detection. In XRF, the detector receives only one wavelength at a time, and therefore provides valuable analytical determinations.

The wavelength-dispersive x-ray fluorescence spectrometer consists of an x-ray generator (x-ray tube and power supply), a specimen chamber and a spectrogoniometer with electronic detection system (Figure 1.3.). The spectrogoniometer has two collimators, an analyzer crystal and a detector arranged on a motor-driven precision rotating mechanism. The collimators consist of spaced parallel metal foils rigidly held in rectilinear metal tunnels. The single crystal bar serves as an x-ray diffraction grating. One collimator is fixed at the output end of the specimen chamber. The crystal is bisected by and rotates about the goniometer axis at angle θ per unit time as the second collimator and detector rotate together at angle 2 θ per unit time.

The constituent elements in the specimen emit their characteristic x-ray spectra in all directions, but only a bundle of rays parallel to the foils of the first collimator reaches the crystal. At each angular position θ, the crystal diffracts only the wavelength λ that satisfies the Bragg law: $2d\sin\theta = n\lambda$, where d is the

interplanar spacing of the crystal planes parallel to the surface and n is an integer defining the diffraction order.

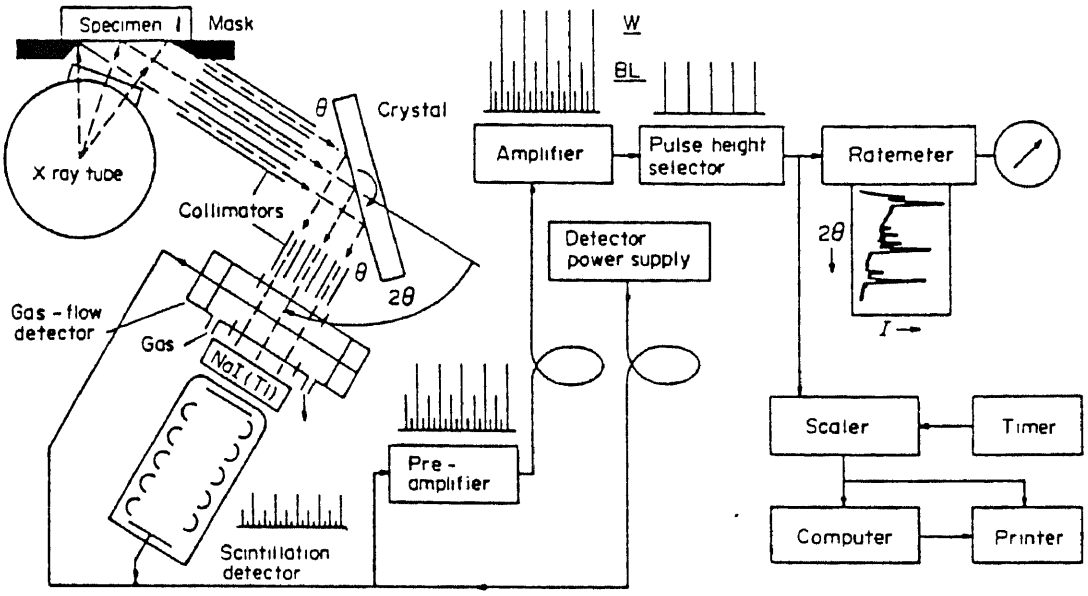

Figure 1.3 XRF experimental setup (Ref. 1).

1.5.3.2 X-ray Diffraction (XRD) X-ray powder diffraction has played a very important role in the development of science and technology. It has become the indispensable method for identifying crystalline phases of inorganic (metal and alloy) and organic (polymer and biological) materials. The major uses of the x-ray powder method are:

1. identifying crystalline phases in solids including qualitative and quantitative analysis of mixtures of phases,

2. distinguishing between mixtures, various types of solid solutions and polymorphs,
3. distinguishing between the amorphous and crystalline states in solids,
4. precision measurements of lattice parameters and thermal expansion, and
5. determining the degree of preferred orientation and crystalline texture.

In the powder diffraction method, x-rays from an x-ray tube strike the target and diffraction will occur if the conditions of the Bragg law are fulfilled. These conditions are defined by the following expression:

$$2d\sin\theta = n\lambda \qquad (1.1)$$

where,

d = spacing between interatomic parallel planes

θ= angle between incident collimated x-ray beam and an atomic lattice plane

λ = wavelength of the characteristic line (usually the CuKa doublet at 0.1540562 nm).

Since the wavelength of the x-ray beam stays fixed, only 2 parameters can change, d and θ. In an x-ray powder diffractometer, the angle between the incident beam and the specimen is changed. For certain angles there is a spacing d, typical for the specimen, where reflection occurs according to Bragg's law. Since no two crystalline phases have the same spacing of interatomic planes in three dimensions, the angles at which diffraction occurs can be used for phase identification.

A focusing x-ray diffractometer with counter detector is normally used. The basic arrangement of the instrument is shown in Figure 1.4. The curved monochromator is usually highly oriented pyrolytic graphite that reflects about 50 % CuKa. It is set to reflect only the Ka doublet and eliminates all other wavelengths from the x-ray tube and specimen fluorescence. The detector rotates around point O at twice the angular speed of the specimen so that the specimen surface is always at θ and the receiving slit at 2θ. The diffractometer is driven by a synchronous motor and the intensities are recorded with a rate meter and strip chart. The intensities and 2θ values are read from the chart and the lattice spacings are calculated from the Bragg equation.

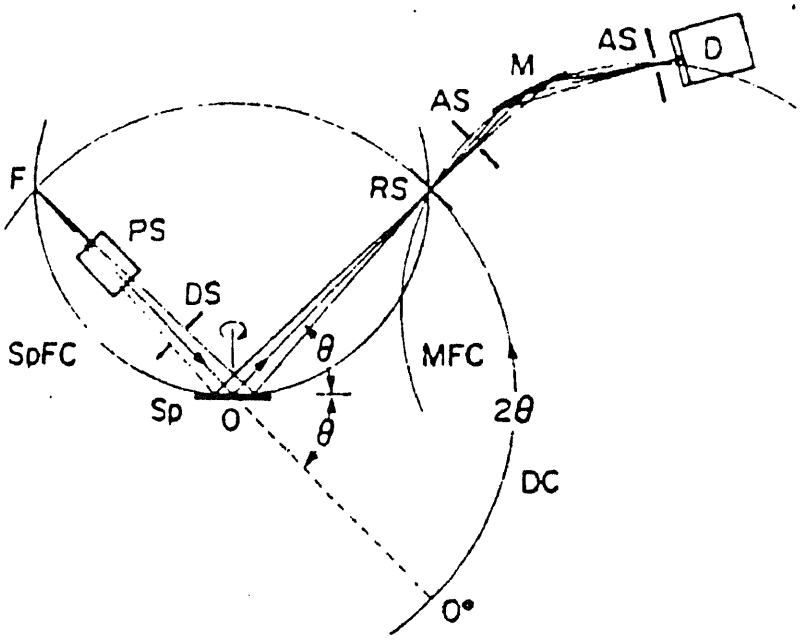

Figure 1.4 XRD experimental setup (Ref. 1).

The powder pattern is a set of reflections in which the lattice spacings and the relative intensities are unique for each crystalline substance. It is this property that makes it possible to identify a substance by comparing its pattern with that of a known substance.

Patterns of mixtures are superimposed individual patterns. In this case the identification of the different substances contained in the mixture becomes more difficult than when one single substance is identified. Every substance is identified separately and when a match is found with a known substance, its pattern is subtracted from the total mixture pattern. This procedure is repeated until every peak in the pattern is identified with a known substance.

1.5.3.3 X-ray Photoelectron Spectroscopy (XPS) In XPS a monochromatic soft x-ray beam (1-5 keV) strikes the material to be studied and the kinetic energy spectrum of the resulting photoemitted electrons is analyzed by an electron spectrometer. Each x-ray photon is usually completely absorbed by a single core electron in the surface of the sample, providing enough energy to let the electron escape from the atom. The kinetic energy of the escaping electron is:

$$E = h\nu - E_b \qquad (1.2)$$

where E_b is the binding energy of the electron in the atom and $h\nu$ is the x-ray photon energy.

If the incident x-ray energy is known and kinetic energy of the escaping electron is measured, the binding energy of the photoelectron can be calculated

from equation 1.2. Since each element has a unique set of binding energies for its core electrons, this binding energy will in turn determine the element from which the electron came. Tabulation of sets of binding energies is given for some specific elements in Table 1.3. These binding energies can be calculated with reasonable accuracy from single-atom models or determined experimentally from x-ray adsorption or emission measurements.

Table 1.3 Binding energies (eV).

	Atomic orbital						
Element	$1s_{1/2}$	$2\ s_{1/2}$	$2p_{1/2}$	$2p_{3/2}$	$3\ s_{1/2}$	$3p_{1/2}$	$3p_{3/2}$
C	284			5			
O	532	24		7			
Al		118	74	73	1		
Si		149	100	99	8	3	
Ca	438	350	347	44	26		5
Cr	695	584	575	74	43		2
Fe	846	723	710	95	56		6

One of the most valuable features of XPS from an analytical point of view is its ability to distinguish between different chemical bonding configurations as well as different elements. This is possible because the binding energies of electrons in an atom are related to the atom's chemical environment. The amount by which the binding energy of a particular line differs from some reference value is termed its chemical shift. This chemical shift is roughly proportional to the electronegativity or valence state of the atom. Due to this

property, XPS can distinguish the chromium valence states, Cr(III) and Cr(VI), if they are present within the detection limit of the technique.

Another important aspect of XPS from the standpoint of an analytical technique is its ability to quantify the spectra obtained. It is possible to determine the relative abundance of the constituents present on the surface by measuring the number of photoelectrons detected in an XPS line of each constituent.

The basic XPS spectrometer consists of an x-ray source for sample excitation, an electron spectrometer to discriminate electron energies and a detection system that produces the XPS spectrum, all mounted in a single vacuum enclosure as depicted in Figure 1.5.

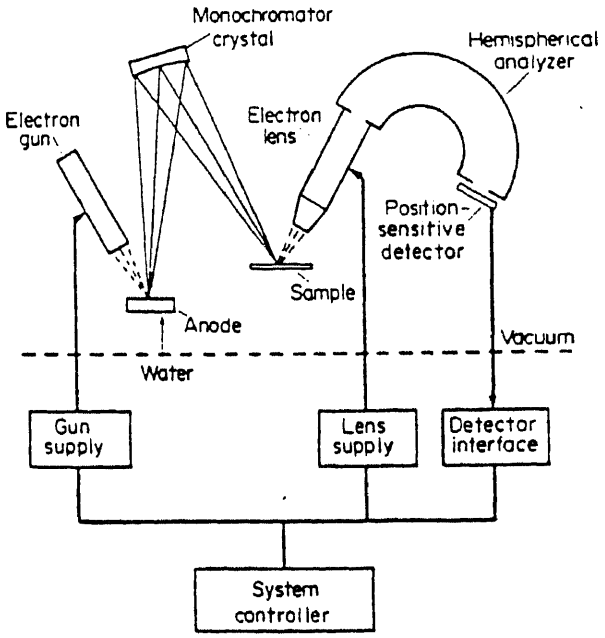

Figure 1.5 XPS experimental setup (Ref. 1).

1.5.3.4 Scanning Electron Microscopy (SEM) - Energy Dispersive X-ray Spectroscopy (EDS) The basic principle of the scanning electron microscope is to scan a specimen with a finely focused electron beam of kilovolt energy. An image is formed by scanning a cathode-ray tube in synchronism with the beam (Figure 1.6) and by modulating the brightness of this tube with beam-excited signals. In this way, an image is built up point-by-point which shows the variations in the generation and collection efficiency of the chosen signal at different points in the specimen.

Unlike the transmission electron microscope, there is no need to refocus the signal-carrying particles generated in the specimen. This makes it possible to examine rough solid specimens with a minimum of specimen preparation. By using different conditions and position of the specimen, it is possible to obtain images showing the surface topography, average atomic number, surface-potential distribution, magnetic domains, crystal orientation and crystal defects in a solid specimen.

An SEM can also be used with an energy-dispersive x-ray detector (EDS) (Figure 1.7). In EDS, x-rays from the specimen enter the intrinsic region of a reverse-biased single-crystal silicon p-i-n device causing the ejection of a photoelectron. The photoelectron then produces a number of electron-hole pairs that are swept away by the applied bias and the total charge is converted to a voltage pulse by a low noise amplifier. The voltage pulse is further amplified by a main amplifier and then processed by a multichannel analyzer (MCA). Since the voltage of each pulse is proportional to the initial x-ray energy, over the course

of the data-collection time a plot of x-ray intensity versus energy appears on the display of the MCA. Peak identification can then be performed rather simply using specially displayed elemental-spectral-line markers which are readily available on almost all computer-based MCA's. These systems also include software packages for peak integration, background subtraction and even full quantitative analysis.

EDS has been broadly used with electron beam instruments. The reason revolves around speed and convenience. With virtually no moving parts and no special focusing requirements the detector crystal can be located very close to the sample, resulting in a much higher collection efficiency. Furthermore, since each pulse is processed as it is received, pulses of one energy are not ignored while the spectrometer is tuned to a different energy (wavelength). These two factors make it possible to rapidly collect x-ray spectra even with the low beam currents of SEM-imaging conditions. Combining this speed with some of the computer-based MCA features, already mentioned, it is often possible to perform a survey qualitative analysis in a matter of a few minutes.

Another interesting feature of the EDS is that it can be used to show the two-dimensional distribution of one or more elements and the corresponding microstructure as seen by the SEM. The elemental maps are obtained by coupling the output of the single channel analyzer to the "brightness" input of the display. Each time a pulse is detected, it is displayed as a dot on the two-dimensional map.

The experimental setups of SEM and EDS are given in Figure 1.6 and 1.7 respectively.

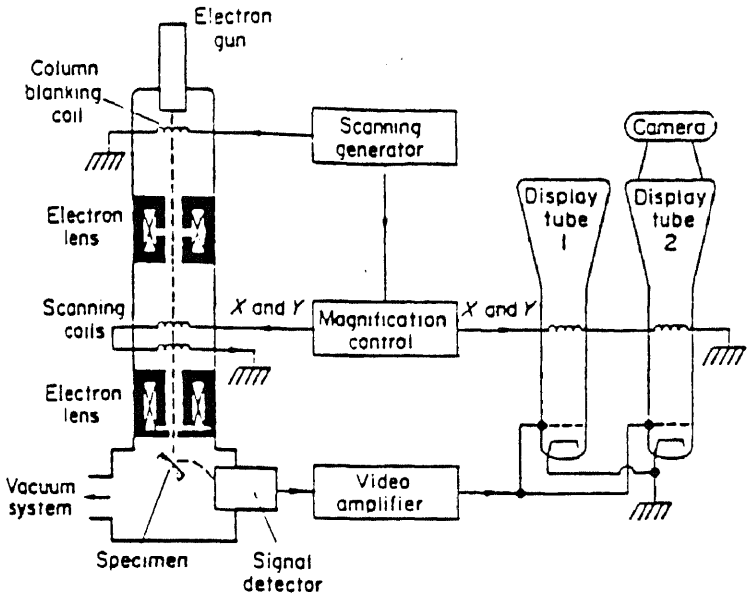

Figure 1.6 SEM experimental setup (Ref. 1).

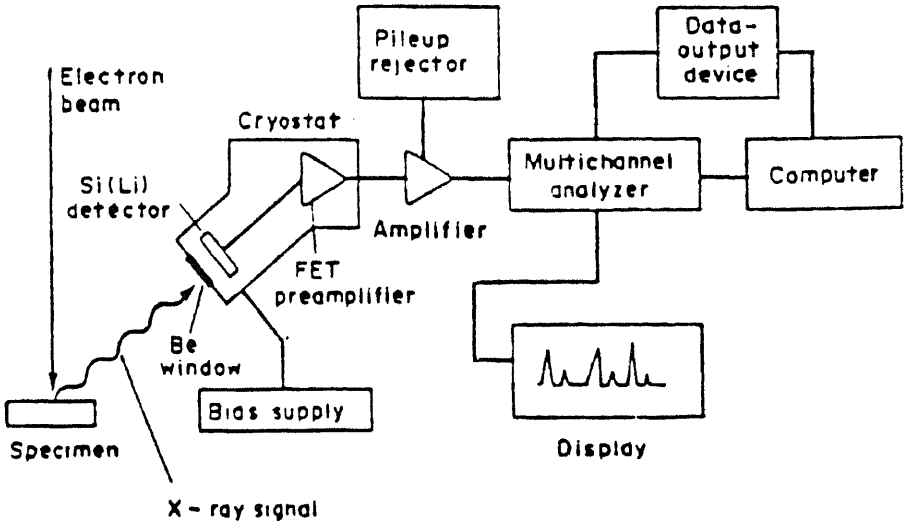

Figure 1.7 EDS experimental setup (Ref. 1).

1.6 Objectives of the Work

There are two major objectives of this research work. They are the following:

1. To apply advanced techniques to characterize heavy metal containing waste, specifically chromium, and to advance the state of the art of the characterization of earth and geotechnical materials, and
2. To use the details and rigorous knowledge of the chromium residue fill generated by advanced characterization to develop treatment technologies, and to understand the impact of this type of waste on the environment

One of the basic challenges in the case of chromium is due to the fact that it is present in two valence states, Cr(III) to Cr(VI). Conventional analytical methods to determine the ratio of Cr(III) and Cr(VI) in waste samples are difficult due to the presence of other elements in the waste that may lead to inter-conversion between the two valence states during wet digestion. Our basic objective in this research is to use XPS to determine Cr(III)/Cr(VI) in the solid state without special sample preparation, i.e., we use the sample as-received from the site. This non-invasive type of analysis guarantees accurate definition of the Cr as it is present in the site.

In addition to XPS, we planned to gain as much information as possible about the waste materials. For this reason, we employed XRD, XRF, SEM, XPS, and EDS. The knowledge (and information) generated from the above techniques demanded special skills that we were able to develop during the research.

To accomplish the second objective, we pursued a new approach to study the waste, to develop treatment methods to remove Cr(VI) and Cr(III), and to determine how Cr valence states may behave in the environment. For this purpose, we studied the electrochemistry of chromium in the waste and defined that the pH, and oxidation potential are the major variables that may affect the ratio of the two valence states (Cr(III)/Cr(VI) in the environment. During the work, we developed and used mathematical models to understand the processes taking place during leaching of Cr(VI). One key objective of the thesis was to understand the process of oxidative dissolution of Cr(III), and to use such process to remove accessible Cr(III) from the waste materials. The results of this work may have important implications of how to deal with chromium-contaminated waste, and how to treat such waste efficiently.

1.7 Organization of the Thesis

In Chapter 2 we discuss the materials and experimental procedures used and developed during this research.

In Chapter 3 we will present the results of advanced characterization of chromium waste fill material. Results of different characterization techniques are discussed to understand the waste material and to develop treatment procedures.

Chapter 4 describes our efforts in the leaching of the hexavalent form of the chromium. Different electrolytes, such as chloride, sulfate, phosphate and

bifluoride were used to leach Cr(VI) from waste. Equilibrium conditions and kinetics of this leaching process are examined and discussed in this chapter. Models were developed to explain the experimental results. Based on our results a process was developed to remove all the accessible Cr(VI) from the waste.

In Chapter 5 we studied the process of oxidative dissolution of Cr(III). After removal of all the Cr(VI), we attempted to oxidize the remaining Cr(III) to the hexavalent form by adding a selection of oxidants (with different oxidizing power) to the leaching solution. For each oxidant different experiments were conducted at different pH conditions. In each experiment, the pH was held constant, such that only the Eh could change depending on the type and concentration of the oxidant that was used. Application of this made it possible to study the influence of pH and Eh separately. The experiments have shown that it is possible to oxidize Cr(III) to Cr(VI) under moderate conditions. This implies that trivalent chromium may become toxic under some conditions since it transforms to Cr(VI) that can be leached into the environment, or may cause chronic effects if inhaled as particles.

In Chapter 6 the conclusions drawn from the above research work are given.

CHAPTER 2

EXPERIMENTAL PROCEDURES

2.1 Description of the Waste Sample

The sample used in our research was obtained from a chromium waste landfill in Hudson County, New Jersey. The material in the landfill is a mixture of a residue from a chromium processing facility, debris and sediment. The sample has a wide particle size distribution ranging from a few microns up to almost an inch. When water is added to the sample, a high concentration of chromate is leached. This is manifested by the yellow-green color of the solution. The pH of the leachate is usually between 11 and 11.5 and the Eh (oxidation potential) is around 300 mV. The total chromium concentration in this waste residue is 20,300 ppm or 2.03 % by weight as determined by Atomic Adsorption following acid digestion and dilution (EPA Method 3050).

In order to obtain consistent experimental results throughout the research, the as-received sample was ground to obtain uniform waste sample. The grinding was performed with a Continuous Ball Mill (Preiser/Mineco LC100). The as-received waste sample was loaded in a stationary bowl in batches of 50 g. Eight 1-inch diameter polished steel grinding balls are added to the sample in the stationary bowl having a machined circular track. Finally an upper grinding ring with matching track is rotated at 20 rpm to drive the balls while a fixed load of 64 lbs. is maintained by weighting the motor driven spindle attached to the

upper ring. Each batch of sample was ground for 120 min. After grinding, the particle size distribution ranged from a few μm up to around 50 μm (see Figure 3.5). This ground sample was used during the experimental work of this research.

2.2 Sample Preparation for the Advanced Characterization

To characterize the ground chromium waste, some sample preparation had to be done, especially for XRD as shown in Table 2.1.

Table 2.1 Sample preparation for the advanced characterization.

Characterization Technique	Sample Preparation
XRF	No special sample treatment was required
XRD	In order to obtain a good powder diffraction pattern a correct powder sample should be prepared. The sample has to be sieved through a 200 mesh (75 μm opening) sieve. The portion of the sample that passes through the sieve is packed tightly on a recession with a layer of vacuum grease. Finally the surface is strucked off smooth and leveled with a clean spatula.
XPS	No special sample treatment was required
SEM/EDS	No special sample treatment was required

Some characterization techniques (XPS and SEM/EDS) were also applied for a few well chosen chromium waste samples that were treated with salt leaching and oxidative dissolution. To obtain a dry solid sample, we separated the treated waste from the leachate solution by means of a Buchner funnel. The solid (treated waste) was then dried in the air at room temperature and used for characterization by various techniques.

2.3 Leaching Procedures

2.3.1 Reagents Used in the Leaching Procedures

For the leaching experiments with inorganic salts, the following electrolytes were used: NaCl, Na_2SO_4, Na_2HPO_4, Na_3PO_4, and $NH_4F.HF$. Those salts were chosen in particular because they have diverse properties with respect to the dissolution of Cr(VI) and they are not harmful to the environment.

For the oxidative dissolution, we used the following oxidants: H_2O_2, $KBrO_3$, $Ce(NH_4)_2(NO_3)_6$, and $KMnO_4$. They have diverse oxidation potential and can be easily dissolved in water.

2.3.2 Leaching with Inorganic Salts

The ground waste samples were used in our leaching experiments. For leaching with the salts (electrolytes), we used the following procedure:

1. The required amount of the inorganic salt was dissolved in deionized water and brought into a 1000 ml beaker.
2. The inorganic salt solution was stirred with a magnetic stirrer until complete dissolution of the salt was achieved, i.e., leaching solution was prepared.
3. Under continuous stirring, the ground chromium waste sample was added to the solution. The stirring was maintained for a few minutes at a high speed until uniform mixing was obtained
4. At the end of the leaching experiment the stirring was stopped and the waste particles were left to settle at the bottom of the beaker.

5. After the particles were settled, a sample was taken from the clear leachate (no particles) to determine the concentration of soluble chromium. In our equilibrium experiments, the leachate was left overnight before a sample was taken for analysis. At the time when the sample was taken, the pH and the Eh of the solution were measured and recorded.

For the kinetics experiment, several samples were taken from the leachate at different times ranging from a few minutes to several days, depending on the type of the experiment. The samples that were taken from the leachate were usually small (5 ml). This was done to minimize errors in the experimental results. The total volume of leachate was 500 ml in most experiments.

During the multiple step extraction reaction experiment, the waste had to be recovered after each experiment. To recover the waste, a Buchner funnel was used to filter the waste from the leachate. After each filtration, the filtrate was added to a fresh made salt solution and the next extraction step was performed.

2.3.3 Oxidative Dissolution

In order to study the oxidative dissolution, we tried to separate the effect of the oxidants from other dissolution effects that may take place during the leaching experiments. Therefore, the ground waste samples were pretreated with salt leachings (2 times with Na_2SO_4 and 1 time with $NH_4F.HF$), until all the Cr(VI) was

removed from the waste (as shown in Chapter 4). The only chromium detected in the leachate during the oxidative dissolution can be attributed to Cr(III) that was oxidized to Cr(VI).

The experiments were conducted in the same way as described previously for the leaching experiments with salts, except for the addition of oxidants to the solution. In an aqueous system, the oxidation potential is coupled with the pH by the Nernst equations (2.1, 2.2) which is based on hydrogen and oxygen (Ref. 7). The two dissolved gases theoretically determine the oxidation potential of water.

$$E_0 = 0.000 - 0.0591pH + 0.0295 \log pH_2 \qquad (2.1)$$

$$E_0 = 1.228 - 0.0591pH - 0.0147 \log pO_2 \qquad (2.2)$$

where,

E_0 = oxidation potential of water

pH_2 = partial pressure of H_2

pO_2 = partial pressure of O_2

If an oxidant is added to the solution, the oxidation potential will rise and the pH will go down. In addition to the influence of the oxidation potential, the effect of the pH was also examined during the oxidative dissolution experiments. Before the oxidative dissolution was started, that is before any oxidant was added, the pH was brought to a certain value and it was kept constant for the rest of the experiment as described above.

2.4 Measuring pH and Eh

The pH and Eh were measured with a microcomputer-based pH meter with a Eh measuring mode (JENCO model 6071). A 3-in-1 pH electrode (pH and reference electrode combined with temperature probe, JENCO model 6000 E) was used to determine the pH. The pH meter was dual point calibrated with a standard solutions of pH 7 and 10. During the experiments, the pH meter was regularly calibrated with the pH standards.

An oxidation-reduction potential electrode (ORP electrode) was used for Eh measurements. The ORP electrode is a combination electrode with an Ag/AgCl reference electrode and a platinum (Pt) electrode. Essentially, the measured ORP is the EMF (Electro-Motive-Force) difference between the potential on the platinum band and the potential of the Ag/AgCl reference electrode. Since the standard ORP (Eh) is usually expressed in reference to the normal hydrogen electrode, the Eh of the solution can be calculated by adding algebraically the measured potential and the standard potential of the Ag-AgCl reference electrode (Er). The standard potential of the reference half cell is 202 mV at 25 ^{0} C, and may change slightly with the temperature. The Er values at different temperatures are given in Table 2.2.

Table 2.2 Er values at different temperatures.

Temperature (^{0} C)	Er (mV)
15	209
20	206
25	202
30	198

The ORP electrode accuracy was routinely tested with the quinhydrone test. The oxidation-reduction potential of a quinhydrone solution is pH dependent. By saturating pH buffers with quinhydrone, we can make stable mV standards solutions to use in testing our ORP electrode. Ideal values for some common buffers (saturated with quinhydrone) are listed in Table 2.3. The actual readings in the buffers could vary by 20 mV. However, a clean ORP electrode will give reproducible Δ values (differences between the potentials of the two saturated buffers) of 169 to 177 mV. It is this Δ value that indicates how functional the electrode is.

Table 2.3 Oxidation-reduction potentials of saturated quinhydrone buffers.

Buffer	ORP
4.01 pH	263 mV
7.00 pH	86 mV

2.5 Analysis of the Leachate Samples

The leachate samples were analyzed for chromium by Atomic Absorption Spectrometry. The principle of AA spectrometry is as follows: Atomic Absorption spectrometry makes use of the fact that neutral or ground state atoms of an element can absorb electromagnetic radiation over a series of very narrow, sharply defined wavelengths. The sample, in solution, is aspirated as a fine mist in a flame where it is converted to an atomic vapor. Most of the atoms remain in

the ground state and are therefore capable of adsorbing radiation of a suitable wavelength. This discrete radiation is usually supplied by a hollow cathode lamp, which is a sharp line source consisting of a cathode containing the element to be determined along with a tungsten anode.

When a sufficient voltage is impressed across the electrodes, the filler gas is ionized and the ions are accelerated towards the cathode. As these ions bombard the cathode, they cause the cathode material to sputter and form an atomic vapor in which atoms exist in an excited electronic state. In returning to the ground state, the lines characteristic of the element are emitted and pass through the flame where they may be absorbed by the atomic vapor. Since, generally, only the test element can absorb this radiation, the method becomes very specific in addition to being sensitive.

For our analysis, the leachate samples were analyzed without any form of sample preparation, except for dilution whenever the concentration of the chromium was higher than 5 ppm (upper limit of the linear range). Five chromium standards were made for calibration purposes., ranging from 1 to 5 ppm. The background solution that was used, was deionized water just like the leaching liquid that was used in our experiments. For leachate samples with high salt and oxidant concentrations, we had to work with a Smith Hieftje Background correction in order to get correct results. During the analysis the readings of the AA spectrometer were checked by running the standards in between the

unknown leachate samples. The setup of the spectrometer that was used for our analysis, is given in Table 2.4.

Table 2.4 Setup of the atomic adsorption spectrometer.

Light source	Hollow Cathode
Lamp current: - normal operation - Smith Hieftje	6.0 mA 2.5 mA, signal match to background intensity
Wavelength	357.9 nm
Bandpass	0.5 nm
Burner head	nitrous oxide
Flame description	nitrous oxide-acetylene, fuel rich, red cone
Sensitivity	0.04 μg/ml
Linear range	0-5.0 μg/ml

The chromium concentrations detected by AA spectrometry are concentrations of chromium as an element. This means that the total concentration of all the chromium ions and species that are dissolved in the leachate. For calculation purposes, we made an assumption that this total chromium concentration equals the concentration of Cr(VI) and that there are no Cr(III) ions present in the leachate solution. This assumption is based on the fact that the condition of the solution is situated in the zone of the stability diagram of chromium (Figure 1.2) where only Cr(VI) is present. To demonstrate that this is valid for all the experiments we will refer to the measured pH and Eh values during the experiments.

2.6 General Calculations

The readings of the AA spectrometer are given in ppm. For consistency, the chromium concentrations are converted in mg/g of waste. All the data from different leaching experiments can then be compared with each other. We will clarify this in a numerical example (Table 2.5).

Table 2.5 Numerical example of conversion of chromium concentration.

Waste Added to Solution (g)	Volume of Solution (ml)	AA reading of chromium concentration (ppm or mg/l)	Amount of chromium in solution (mg)	Amount of chromium in solution (mg/g waste)
5	500	4	2	0.4

All the plots were made based on the Cr(VI) concentrations in mg/g of waste. More specific calculations like curve fitting are described in the following chapters.

CHAPTER 3

ADVANCED CHARACTERIZATION OF CHROMIUM WASTE AND SOIL

3.1 Background and Objectives

One major objective of this research is to employ several advanced characterization techniques to gain detailed information about waste materials and specifically to address the chromium contamination problem in the State of New Jersey. The waste material used in our work is the residue of chromium refining operations, obtained from a site in Hudson County, New Jersey.

Conventional environmental analytical methods are mostly concerned with accurately determining the concentration of the chromium contaminants in soils or other media. In contrast, advanced characterization techniques such as XRF, XRD, XPS, SEM, and EDS can provide detailed information about the chromium compounds, chromium valence states and chemical association with the other phases in the waste matrix. This information is vital in understanding the chromium waste, and to how chromium is present in the waste. The objective of this chapter is to present the results of advanced characterization of a chromium waste material, and to describe the information that can be generated by the application of such advanced techniques.

During our work, we used XRF, XRD, XPS, and SEM-EDS analysis. The latter included both spot and digital elemental mapping of chromium waste. Description of these advanced characterization techniques is given in Chapter 1.

The results of advanced characterization are discussed in this chapter. A strategy for performing advanced characterization of complicated waste materials is proposed.

3.2 Materials and Methods

The chromium waste sample used in this work was collected from a landfill in Hudson County, New Jersey. The material in the landfill is a mixture of a residue from a chromium refining facility, debris and sediment. No special pretreatment was required to perform the advanced characterization techniques, except for XRD, as described in Table 2.1.

3.3 Results and Discussion

3.3.1 X-ray Fluorescence Spectroscopy (XRF)

The elemental scan obtained by XRF is useful for the interpretation of x-ray diffraction results. It also gives the basic idea about the waste composition. An accurate elemental scan was obtained (Table 3.1).

Table 3.1 XRF results.

Major Elements (10-100%)	Ca, Fe
Intermediate Elements (5-10%)	Si, Al, S
Minor Elements (1-5%)	Cr, K, Cl, Cu, Ni

3.3.2 X-ray Diffraction (XRD)

Knowledge of the crystalline phases of the waste material is essential in understanding its properties and possible association of heavy metal contaminants with various phases. XRD was applied to the chromium waste fill as it was found on the site. The powder diffraction pattern is shown in Figure 3.1.

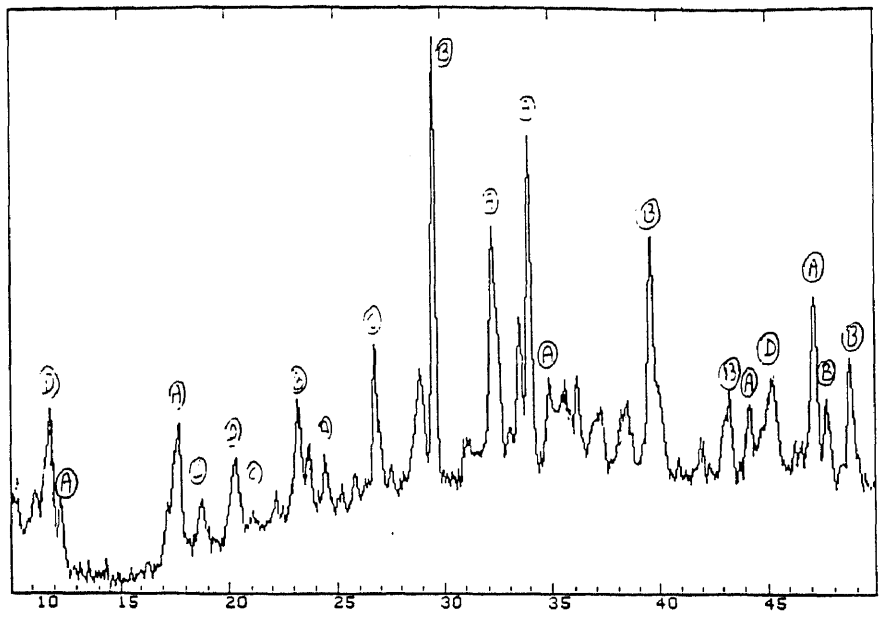

Figure 3.1 Powder diffraction pattern of the chromium waste fill.

The diffraction pattern was found to be very complex. There is a background due to the presence of a small amount of amorphous phases. The crystalline phases listed in Table 3.2 were identified from the powder diffraction pattern. All the crystalline phases found in the waste sample are not typical soil minerals, except for the α-quartz crystal (SiO_2). The results are consistent with the origin of the sample _ a residue of chromium refining operations.

Table 3.2 Waste matrix crystalline phases.

Original sample of chromium residue fill		
Crystalline phase	2θ	Qualitative relative abundance
$Ca_2(Al,Fe)_2O_5$ (orthorombisch)	33.80	major (a) *
$CaCO_3$ (rhombohedral)	29.40	major (b) *
SiO_2 (hexagonal)	26.60	major (c) *
$Ca_4Al_2O_6CO_3.11H_2O$ (triclinic)	11.70	major (d) *
Mn_3O_4	33.80	minor
Fe_2O_3	33.10	minor
$MgAl_2(OH)_8$	18.60	minor
$Mg_4Al_2(OH)_{14}.3H_2O$	11.70	minor
$CaSO_4.2H_2O$	11.60	minor
$Ca(CrO_4).2H_2O$	11.15	minor

(*) The letters a,b,c, and d refer to the peaks in the diffraction pattern (Figure 3.1)

Most of the minerals seem to be made during the processing of the chromium ore (flow diagram of the chromium production is given in Figure 1.1).

The major phase, found in the waste residue is $Ca_2(Al,Fe)_2O_5$, otherwise known as Brownmillerite. This phase is a common phase in Portland cement. Only a very small amount of chromium containing may exists as crystalline phases of this waste matrix.. Our main observations are consistent with:

1. Chromium is present as Cr(VI) in the lattice of the $Ca(CrO_4).2H_2O$ phase, which is only a very minor phase. This was positively identified in the pattern.
2. With respect to the Browmillerite phase, it is possible that some Al(III) or Fe(III) may be substituted by Cr(III) in the lattice. This substitution may take place because the ions (Al(III), Fe(III), and Cr(III)) have the same valance and their ionic radii are almost the same(Table 3.3).

Table 3.3 Ionic radii of Cr(III), Al(III), and Fe(III).

Ion	Radius (A)
Cr(III)	0.62
Al(III)	0.54
Fe(III)	0.55

3.3.3 X-ray Photoelectron Spectroscopy (XPS)

The chromium waste specimens were examined initially by low resolution survey scans to determine elements present in the as-received waste material (Figure 3.2). The sample contained the following elements: Mg, Fe, C, Si, Al, N, Ca, and Cr.

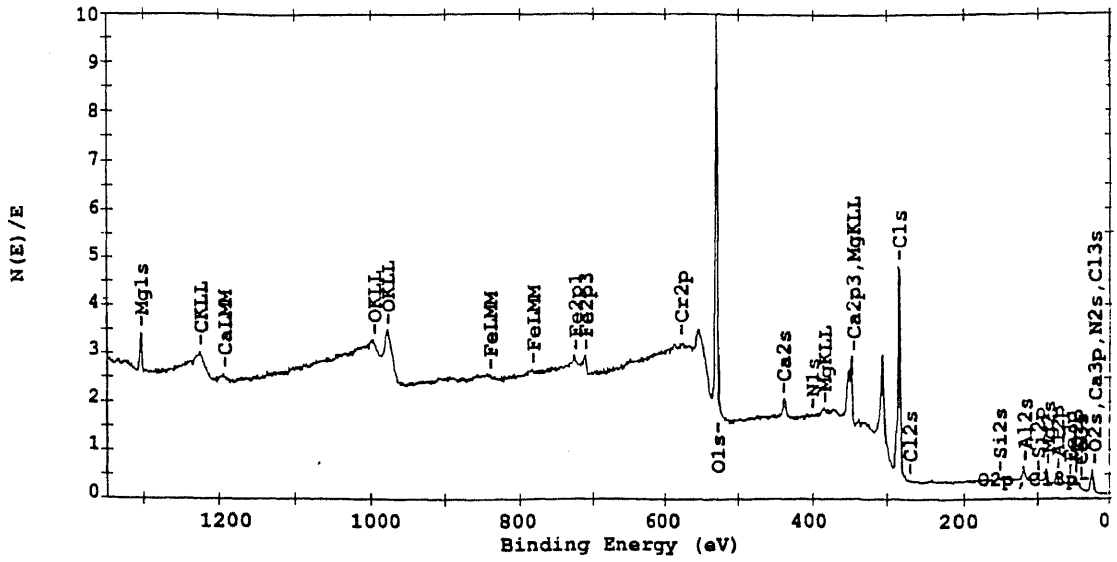

Figure 3.2 Low resolution survey scan.

High resolution spectra were taken to determine the binding energy of the selected elements from the survey scans. The concentration of elements expressed in atom and mass percentage are given in Table 3.4.

Table 3.4 Concentrations of detected elements.

	Mg	Fe	O	C	Si	Al	N	Ca	Cr
atomic %	2.6	1.6	39.2	48.8	0.5	2.7	0.2	4.2	0.3
mass %	3.9	5.5	38.4	35.8	0.9	4.5	0.2	10.3	1.1

Based on this result, the surface of the waste particles contains around 1.1 % or 11,000 ppm chromium. This value (1.1 % by weight) is less than the concentration determined by bulk analysis using EPA method 3050. Most XPS results show abundance of carbon on the material surfaces because of the adsorption of hydrocarbons and other carbon compounds from the atmosphere. It should be noted here that XPS results for total chromium are not reliable due to the presence of high concentrations of adsorbed carbon species on the surface of the particles.

The main reason for using XPS characterization is its ability to determine the concentrations of Cr(III) and Cr(VI) at the surface of the particles in solid state and without the need for chemical digestion. At high resolution, the following chromium spectra were obtained - binding energies between 572-582 eV (Figure 3.3). The acquisition time was about 30 minutes in this case.

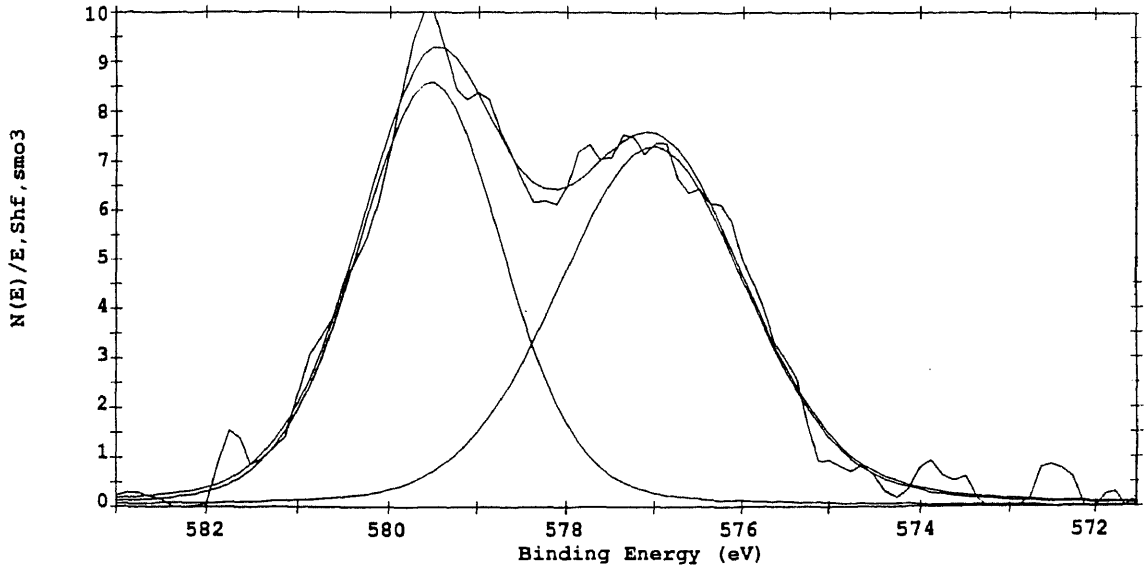

Figure 3.3 XPS spectra for Cr(III) and Cr(VI).

Cr(III) and Cr(VI) have been resolved by XPS in our case. The first band is assigned to Cr(III) (Cr_2O_3 and $Cr(OH)_3$, or its hydrated form, are the most likely species) and the second band is associated with Cr(VI), most likely as CrO_4^{2-}. In order to determine the Cr(III)/Cr(VI) ratio we used a curve fitting routine. The following percentages are assigned to those two bands (Table 3.5):

Table 3.5 Percentages of Cr(III) and Cr(VI) on the surface.

	band	binding energy	percentage
Cr(III)	1	577.03	52.62
Cr(VI)	2	579.54	47.38

The suface of the waste appears to have about 47 % Cr(VI) and 53 % Cr(III). In another sample, we obtained Cr(III)/Cr(VI) of 61/39. The results vary by 10 to 15 %, based on our experience. Based on our analysis with XPS, we believe that the Cr(III)/Cr(VI) determined by XPS is accurate and represent the actual ratio in the bulk of the material. This is because the sample used for XPS analysis was finely ground and the interior of the particles was distributed uniformly in the sample.

3.3.4 Scanning Electron Microscopy (SEM) - Energy Dispersive X-ray Spectroscopy (EDS)

The SEM-EDS techniques were used to determine any likely association between Cr and other elements like Fe, Al and Si in the waste matrix. It can therefore, serve as a powerful speciation tool. Elemental maps were obtained at magnifications of X350, X1000 and X3500. The SEM electron micrographs at magnification X350 and X1000 are given in Figure 3.4, 3.5. Elemental maps at magnification X1000 are given in Fig. 3.6, 3.7, 3.8 and 3.9. The elemental mapping results show a possible association between chromium and aluminum. Except for those few concentrated areas, the chromium in the waste seems to be spread over the whole sample. In other words, the chromium contamination is smeared through out the waste matrix with very few pockets of high chromium concentration.

Figure 3.4 SEM micrograph at magnification X350.

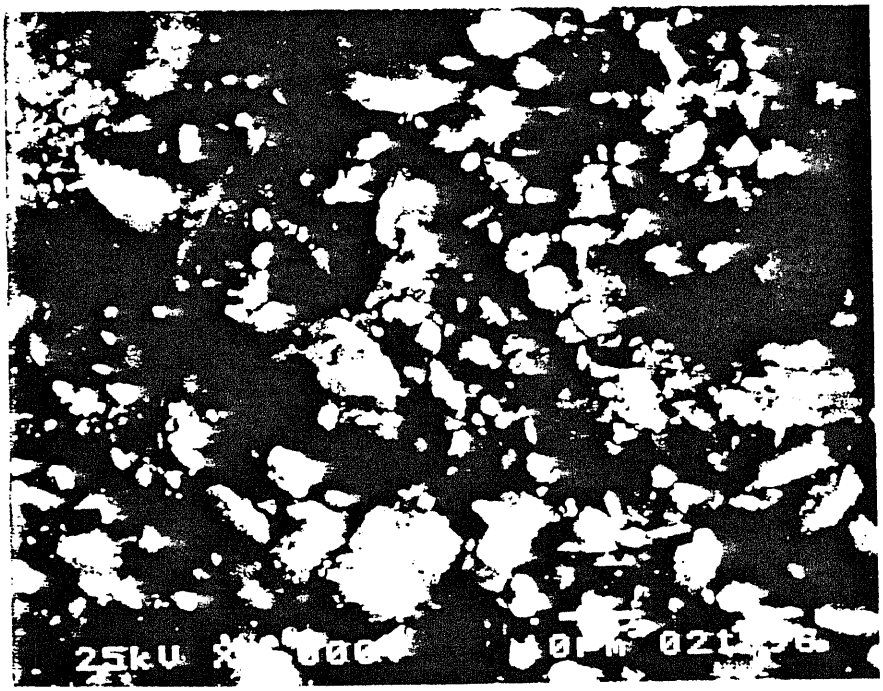

Figure 3.5 SEM micrograph at magnification X1000.

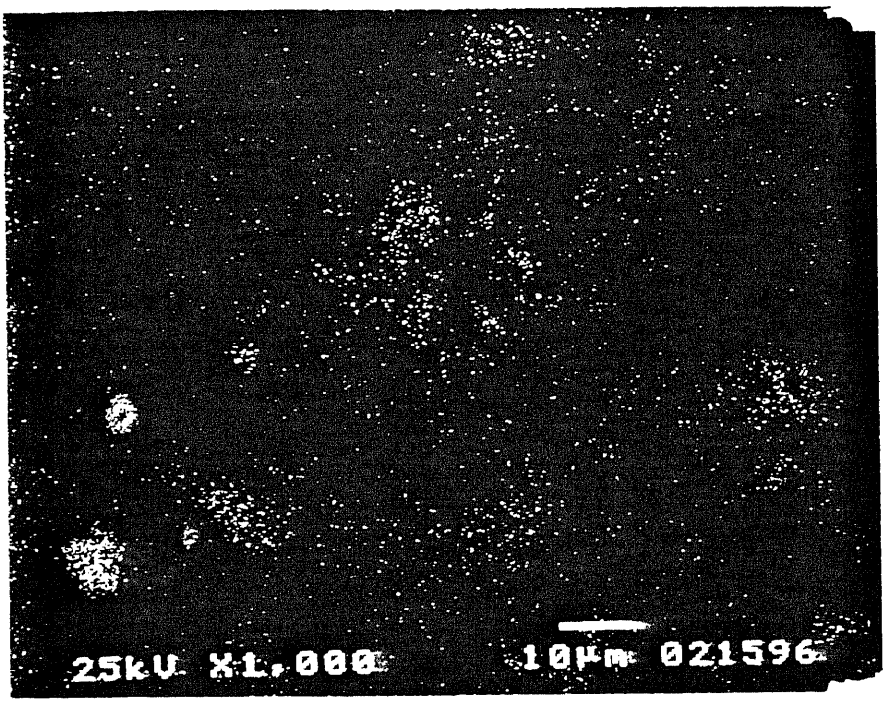

Figure 3.6 EDS Cr map at magnification X1000.

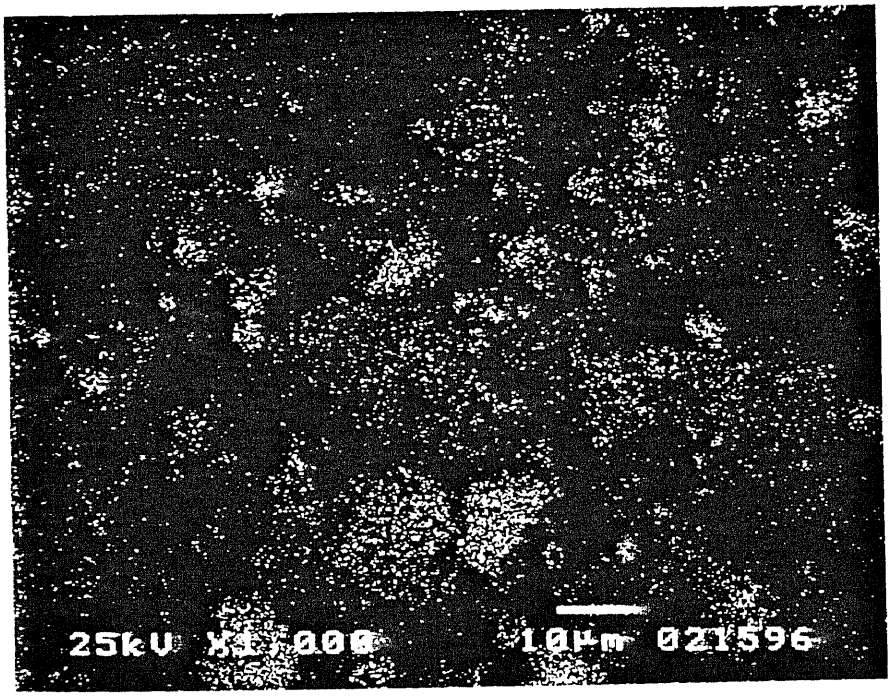

Figure 3.7 Fe EDS map at magnification X1000.

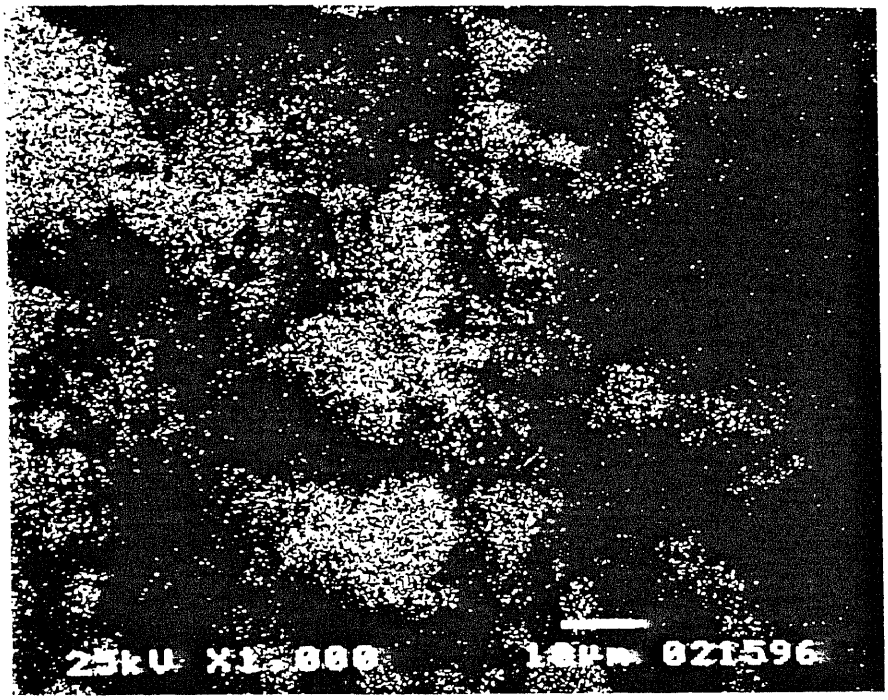

Figure 3.8 Al EDS map at magnification X1000.

Figure 3.9 Si EDS map at magnification X1000.

3.4 Conclusions

Due to the complexity of earth materials, we found that the following strategy for advanced characterization is preferred. Our strategy is based on acquiring the most valuable information at the least possible cost and consisted in employing the analysis in four tiers, as shown in Table 3.6.

Table 3.6 Strategy for advanced characterization

Tier	Used Techniques	Valuable Information Generated
1	XRD, XRF	approximate ratio of crystalline to amorphous phases, major crystalline phases, minor crystalline phases and elemental composition of the samples
2	XPS	surface composition, bonding of various elements, valence states of specific elements (Cr(III)/Cr(VI) in our case)
3	SEM, EDS: spot analysis and elemental mapping	physical distribution of the heavy metal contained in the waste, possible association between elements in the samples (- whether the heavy metal confined to a single phase or distributed throughout the sample)
4	Draw rigorous conclusions and formulate a detailed picture of the waste based on combining the information gathered from tier 1, 2, and 3. This information may include speciation of elements and distribution of contaminants in the matrix. The matrix holding the heavy metal may be identified by combining the results of various characterization techniques.	

In summary, the chromium waste sample used in our studies is a complex mixture of crystalline and amorphous phases. Brownmillerite mineral phase ($Ca_2(Al,Fe)_2O_5$) appears to the major crystalline phase in the waste residue

material. It is possible that some Cr(III) exist in the crystalline lattice of this phase. This remains to be identified by other techniques.

Only one minor crystalline phase was found to contain Cr in its lattice - ($Ca(CrO_4).2H_2O$). The chromium on the surface of the waste particles is definitely present as Cr(III) and Cr(VI) species. The Cr(III)/Cr(VI) ratio was between 53/47 and 61/39 as measured by high resolution XPS. Further the chromium is distributed throughout the waste matrix with some weak association with aluminum.

CHAPTER 4

LEACHING OF CR(VI) FROM WASTE MATERIAL

4.1 Background and Objectives

Based on our XPS results, we have determined that Cr(VI) and Cr(III) are present at the surface of chromium residue materials. We have examined several samples and obtained Cr(III)/ Cr(VI) ratios between 61/39 and 53/47. In this chapter, we present the results of our experiments regarding the leaching of Cr(VI) from these waste samples. In the light of pH and Eh conditions of the waste materials, Cr(VI) is mostly present in the form of CrO_4^{2-}. Since soluble Cr(VI) is toxic and mobile in the environment, understanding of its leaching characteristics and removal from waste is required.

Due to the high concentration of Ca and Mg in this waste material, we assumed that the CrO_4^{2-} anion may be present as counter ions for Ca and Mg sites. Based on this hypothesis we proposed that CrO_4^{2-} may be efficiently leached and released by aqueous solutions containing inorganic anions such as Cl^-, SO_4^{2-}, PO_4^{3-}, and others. This strategy is consistent with desorption and ion exchange processes of CrO_4^{2-} from this waste. In this chapter, we examine the leaching of Cr(VI) from waste with various aqueous inorganic salt solutions. The efficiency of displacing CrO_4^{2-} from solute under equilibrium conditions using various anions is studied. The kinetics of the leaching process of CrO_4^{2-} from

waste is also studied in detail. We present our view of how Cr(VI) is leached from this waste.

4.2 Materials and Methods

All the leaching experiments were performed using ground chromium waste samples, as described in Chapter 2. Based on our XPS analysis of the ground sample used for leaching studies, Cr(III)/ Cr(VI) was 61/39. Leaching solutions were added to the chromium waste samples and initially mixed by stirring for a few minutes. Leachate samples were taken at different time intervals for AA analysis. Leachate samples were separated either by filtration or decantation of the clear leachates. Different inorganic salt solutions were used to study the leaching of the chromate anion from the waste (Table 4.1).

Table 4.1 Salt solutions used in the Leaching Experiments.

Salt	Valence of Anion
NaCl	1
Na_2SO_4	2
Na_3PO_4	3
$NH_4F.HF$	1

4.3 Results and Discussion

4.3.1 Oxidation-Reduction Potential (Eh) and pH of Leachate Solutions

The Eh and the pH of the leachate solution are two important parameters, that were monitored during our leaching experiments. Knowledge of both parameters is required to define the leaching conditions in the potential (Eh)-pH equilibrium diagram - also known as the Pourbaix diagram (Ref. 8) (Figure 4.1). From the Pourbaix diagram we should be able to define which chromium species are stable under our experimental conditions.

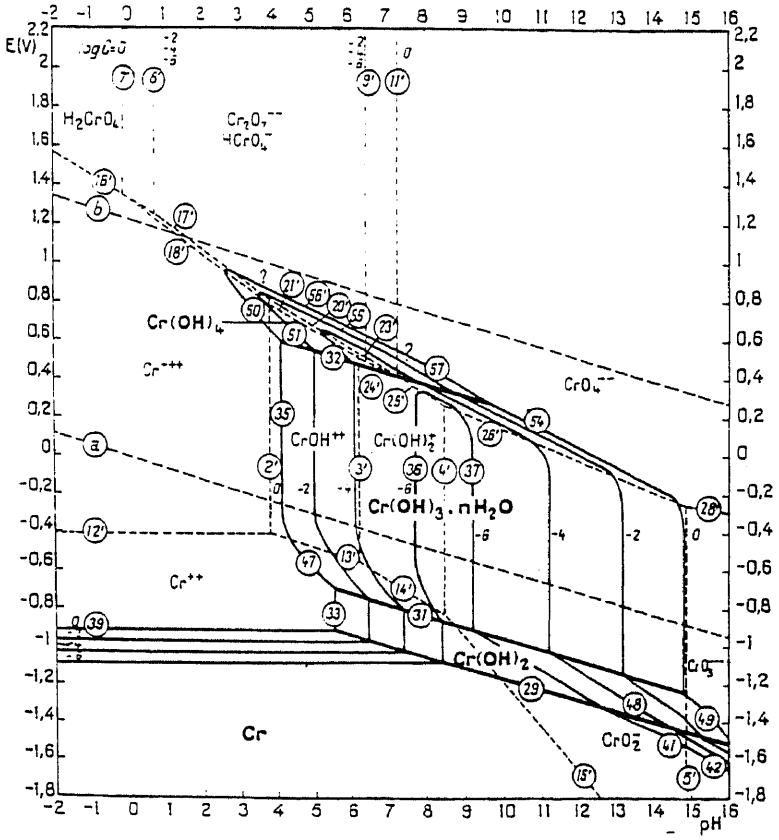

Figure 4.1 Potential-pH diagram for the system chromium-water, at 25 ^{o} C.

To define such electrochemical conditions, we determined the Eh and pH of the deionized water used in the leaching experiments. We selected three random samples of deionized water for this analysis. The following Eh and pH values were measured for each of them (Table 4.2).

Table 4.2 Eh and pH of different deionized water supplies.

supply	pH	Eh (mV)
1	5.7	465
2	4.9	525
3	5.2	507

The water used in our experiments was slightly acidic (because of adsorbed CO_2 from air) and oxidative. Also the Eh and pH of the frequently used salt solutions were measured (Table 4.3). The concentration of the salts was 0.1 mol/l.

Table 4.3 Measured Eh and pH of solutions with NaCl, Na_2SO_4 and Na_3PO_4.

	NaCl		Na_2SO_4		Na_3PO_4	
time (min.)	pH	Eh (mV)	pH	Eh (mV)	pH	Eh (mV)
5	5.3	449	8.3	408	11.9	183
40	6.7	458	8.3	417	11.9	202

The pH is regulated by the salt in the solution. The pH values for each of these 0.1 M salt solutions were calculated using proton balances (equations 4.1 for NaCl, 4.2 for Na_2SO_4, and 4.3 for Na_3PO_4).

$$[H^+] + [HCl] = [OH^-] \quad (4.1)$$

$$[H^+] + [HSO_4^-] + 2[H_2SO_4] = [OH^-] \quad (4.2)$$

$$[H^+] + [HPO_4^{2-}] + 2[H_2PO_4] + 3[H_3PO_4] = [OH^-] \quad (4.3)$$

Based on those proton balances pH-concentration diagrams were constructed for each of the salt solutions and the following pH values were obtained (Table 4.4).

Table 4.4 Calculated pH of solutions made with NaCl, Na_2SO_4 and Na_3PO_4.

salt	NaCl	Na_2SO_4	Na_3PO_4
pH	7	7.5	12.7

Except for the NaCl salt solution, the calculated and the measured pH values are comparable. For NaCl we have a higher calculated pH value, because a) we added the NaCl to water with a pH of 5.7 instead of 7 (for the calculation based on the pH-concentration diagrams we assumed that the salts are added to water with a pH of 7),and b) adding Cl^- has no influence on the pH.

To further define our experimental conditions, we measured the Eh and pH of various leachate solutions after we added our chromium waste (Table 4.5).

Table 4.5 Eh and pH of the leachate solution after waste is added.

	NaCl (0.1 M)		Na_2SO_4 (0.1 M)		Na_3PO_4 (0.1 M)	
time (min)	pH	Eh (mV)	pH	Eh (mV)	pH	Eh (mV)
0	10.4	284	10.6	296	12	206
30	10.5	279	10.6	287	11.9	212
90	10.4	279	10.6	288	11.9	213
1440	10.4	340	10.5	321	12	214

After the chromium waste is added, the pH increased in all cases. When water is added to the waste we measured a pH of 11.3 and Eh of 293 mV. The waste material is very alkaline and, once the waste is added, the type of salt has no significant influence on the pH of the leaching solution. It is important to note that, the Eh and pH of the suspension (chromium waste + salt solution) determine a point in the Pourbaix diagram (Figure 4.1) where CrO_4^{2-} is the stable chromium specie, regardless of the type of leaching salt solution used. In the light of this finding, we can exclude the possibility of the reduction of CrO_4^{2-} to Cr(III) species during our leaching experiments. On the other hand, because of the slightly oxidizing conditions, it should be taken into account that Cr(III) can be converted to Cr(VI) followed by the leaching of the latter in the solution; this is possible under acid conditions only. As will be pointed out in Chapter 5, the amount of Cr(III) leached from the waste in the solution by oxidative dissolution is very small (a few % of the total chromium in the waste residue). Notice that the latter discussion only contained the following salts : NaCl, Na_2SO_4 and Na_3PO_4. We conducted one more experiment with $NH_4F.HF$. We measured the following Eh and pH values after this salt solution was added to the waste residue (Table 4.6).

Table 4.6 Eh and pH of $NH_4F.HF$ 0.1 M solution after waste was added.

$NH_4F.HF$	
Eh (mV)	pH
758	5.11

The Eh and pH of this suspension (chromium waste + salt solution) also determine a point in the Pourbaix diagram (Figure 4.1) where $HCrO_4^-$ is the stable chromium specie.

4.3.2 Effect of the Leaching Solution Volume on the Leaching of Cr(VI)

We added different volumes of 0.001 M salt solutions to 10 g of our chromium waste sample and examined the leaching efficiency by analyzing the Cr in the leachate. The following volumes were used in these experiments (Table 4.7).

Table 4.7 Volumes used to study the effect of volume on the Cr(VI) removal.

volume (ml)
25
50
100
250
1000
2000
5000

The Cr(VI) removed from the waste as a function of the leachate volume is given in Figure 4.2. This experiment was done to find the volume/waste ratio where the chromium removal reaches a plateau value (equilibrium). It was found that a plateau value is reached for all of the studied salt solutions at a volume/waste ratio of 500 ml/g. We choose a salt concentration of 0.001 M, because this is the lowest concentration used in the future experiments.

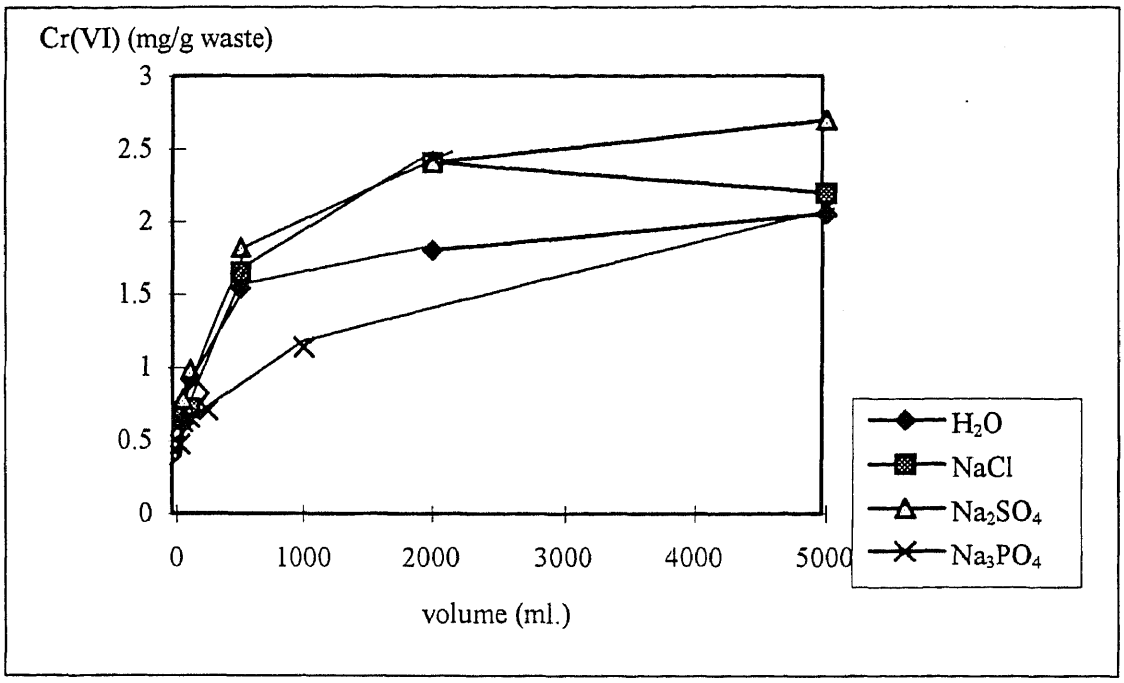

Figure 4.2 Influence of leaching volume on the Cr(VI) removal.

At a higher salt concentration the plateau value will be reached at a lower volume/waste ratio. Therefore, at a volume/waste ratio of 500 ml/g, all our experiments will be conducted under conditions where the effect of volume on the leaching of the Cr(VI) can be excluded.

4.3.3 Influence of Electrolyte Concentration on the Leaching of Cr(VI)

To study the influence of salt concentration on the Cr(VI) removal we conducted a series of leaching experiments with 1000 ml salt solution added to 2 g of chromium waste. The concentrations that were used in the experiments are given in Table 4.8.

Table 4.8 Concentrations used to study the effect of electrolyte concentration on the Cr(VI) leaching from waste.

concentration (mol/l)
0.001
0.01
0.1
0.2
0.5
1

The Cr(VI) removed from the waste as a function of the salt concentration is given in Figure 4.3. The following salts were used: Na_3PO_4, Na_2SO_4 and NaCl.

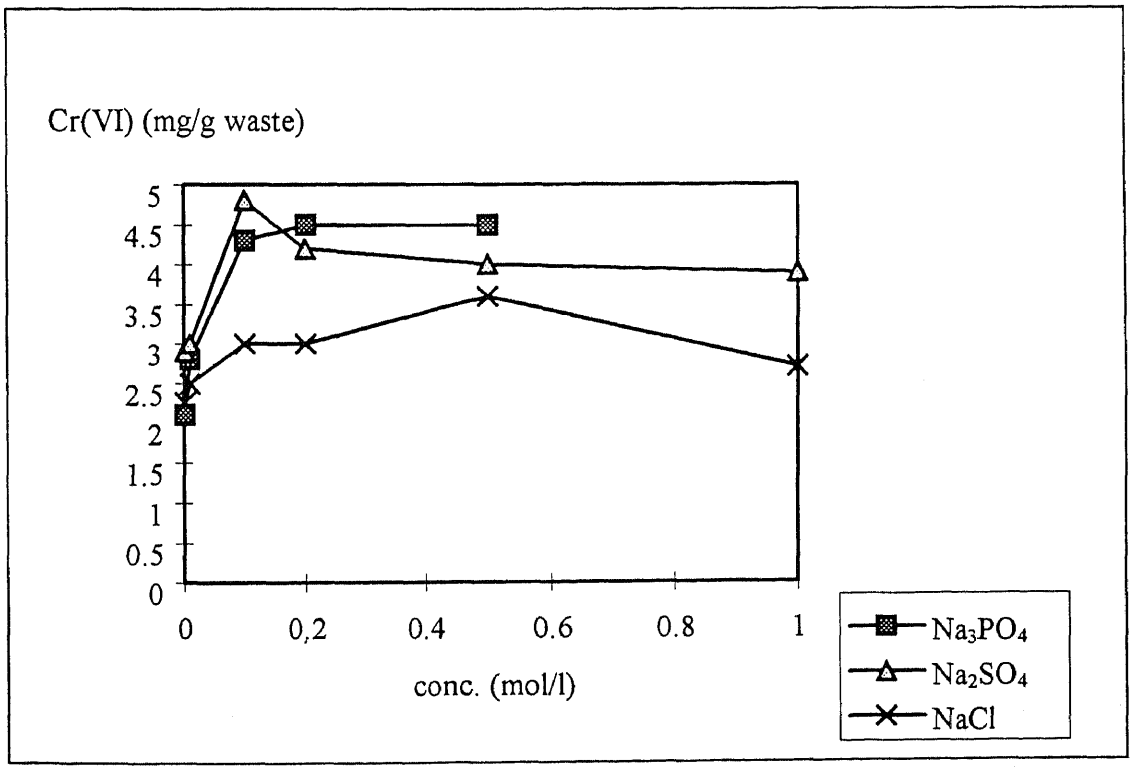

Figure 4.3 Influence of salt concentration on the Cr(VI) removal.

At a certain electrolyte concentration a plateau value is reached, and the maximum removal of Cr(VI) from the chromium waste can be calculated. If the concentration of electrolyte is increased, the number of sites that are occupied by the salt anions will increase.

4.3.4 Influence of the Type of Salt on the Leaching of Cr(VI)

Figure 4.3 shows different amounts of Cr(VI) removed for the different salts used in the experiment. To allow a meaningful comparison between the different salt solutions, we introduce removal efficiencies, defined as mg of Cr(VI) removed per g of waste when the plateau value is reached as shown in Figure 4.3. The removal efficiencies of the studied salt solutions are given in Table 4.9.

Table 4.9 Removal efficiencies for different salts.

salt	Valence of the anion	removal efficiency (mg/g waste)
NaCl	1	3
Na_2SO_4	2	4
Na_3PO_4	3	4.5

NaCl, Na_2SO_4 and Na_3PO_4 follow the rule that the number of adsorbed anions (and therefore the number of removed chromate ions) increases with the valence of the anion. The same principle has been studied for coagulation processes, where it is usually associated with the Shultz-Hardy rule (Ref. 5). This rule stipulates that the critical coagulation concentration (c.c.c.) varies with the valence z of the counter-ion as

$$c.c.c \sim z^{-n} \qquad (4.1)$$

where the exponent n can be 6 or 2. The higher the valence of the counterion, the more efficient is the salt in decreasing the surface charge of particles. In our case, the salt anions function as counterions for the dubble layer at the interface between waste particles and the solution.

In a separate experiment, the effect of $NH_4F.HF$ on the amount of chromium leached out from the waste was studied (Figure 4.4). $NH_4F.HF$ has a high removal efficiency which we attribute to the fact that $NH_4F.HF$ reacts with the waste material and decreases the pH to 5.

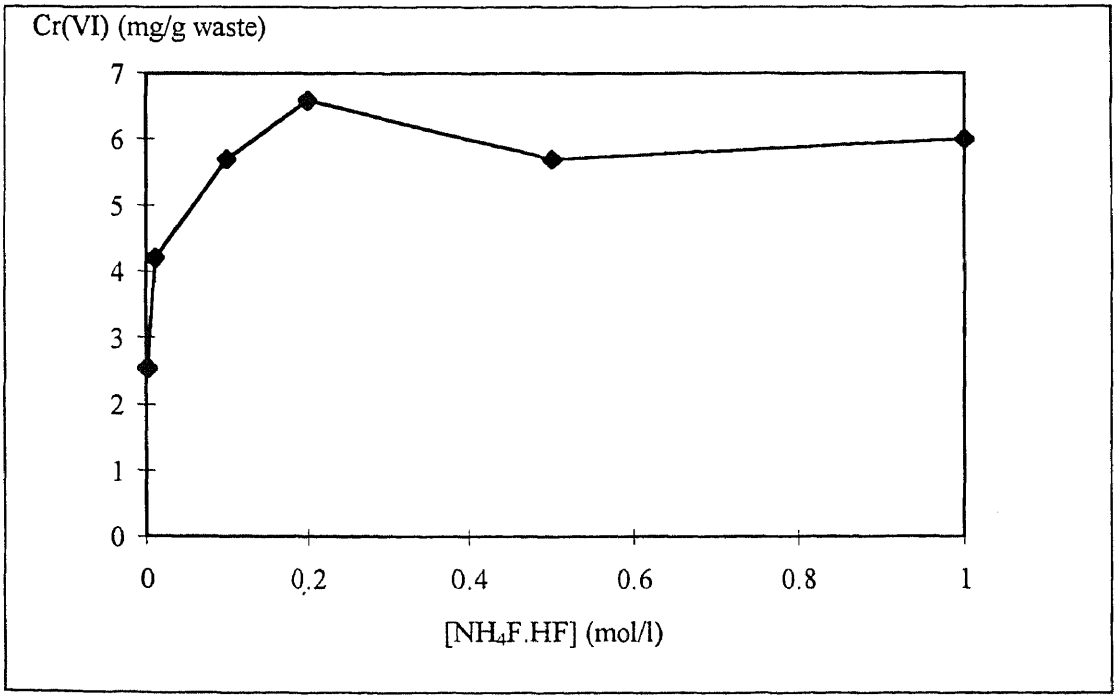

Figure 4.4 Influence of the $NH_4F.HF$ concentration on the Cr(VI) removal.

4.3.5 Kinetics of the Cr(VI) Removal

We studied the kinetics of the chromate removal for four leaching solutions:

1. pure deionized water
2. 0.1 M NaCl solution
3. 0.1 M Na_2SO_4 solution
4. 0.1 M Na_3PO_4 solution

A leachate volume of 500 ml. was added to 5 g. of chromium waste. Samples were taken from the leachate starting at 10 min. up to several days. The results are presented in Figure 4.5.

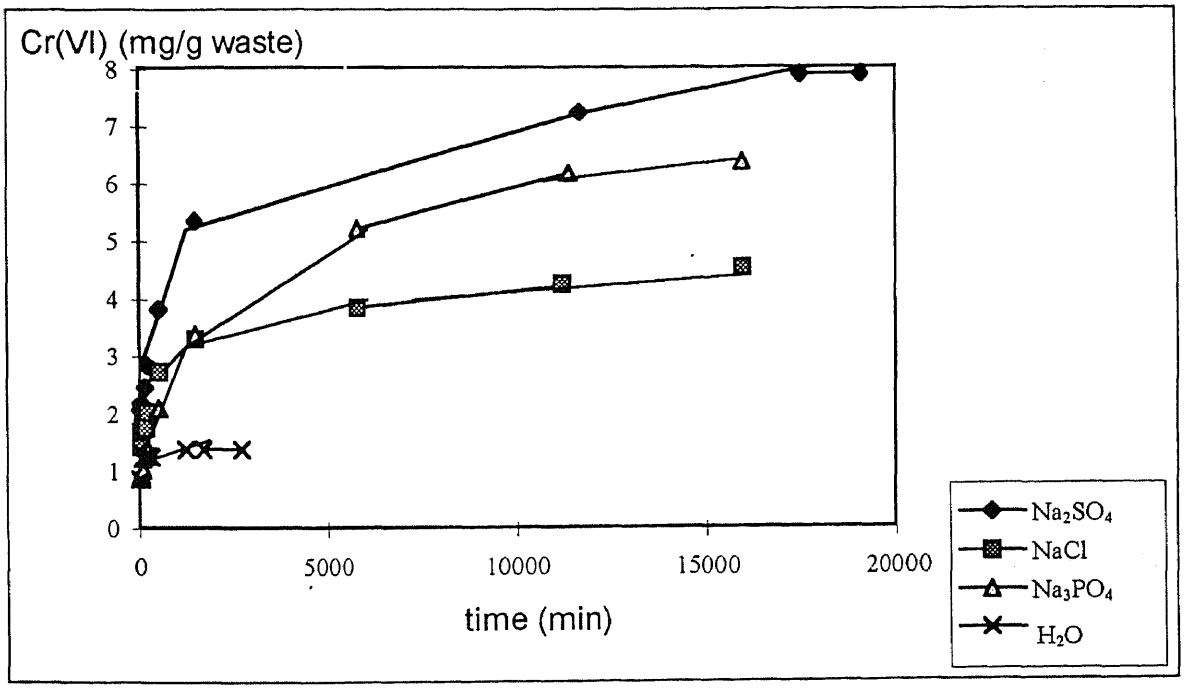

Figure 4.5 Kinetics of chromium removal.

The Cr(VI) removed from the waste reached a maximum that was different for each of the salts anions in the leachate. The maximum removal values are given in Table 4.10.

Table 4.10 Maximum Cr(VI) removed for different leaching solutions.

Leaching solution	Max. Cr(VI) removal (mg/ g waste)	Max. Cr(VI) removal (% of total Cr in waste)
pure deionized water	1.40	6.9
0.1 M NaCl solution	4.55	22.4
0.1 M Na_2SO_4 solution	7.92	39.1
0.1 M Na_3PO_4 solution	6.38	31.5

It should be noted that the Na_2SO_4 solution has the highest removal efficiency. When we studied the influence of the concentration, it was found that the Na_3PO_4 solution has the highest efficiency because of the high valence of the phosphate ion. The reason why this is different for this case is not known. With the Na_2SO_4 solution we were able to remove 39 % of the total chromium in the waste, which equals the total amount of Cr(VI) on the surface of the waste particles determined by XPS analysis.

The data were fitted with equation 4.3, which describes the mass transfer process shown in Figure 4.6. It is of first order in the mass of Cr(VI) released in the solution.

$$dq/dt = -k_r q + k_f(q_\infty - q) \qquad (4.3)$$

where,

q = mass of Cr(VI) released in the leaching solution [mg/g waste],

t = time [min.],

k_r = reverse rate constant, transfer from solution to waste [1/min.],

k_f = forward rate constant, transfer from waste to solution [1/min.], and

q_∞ = max mass of Cr(VI) released in the leaching solution [mg/g waste].

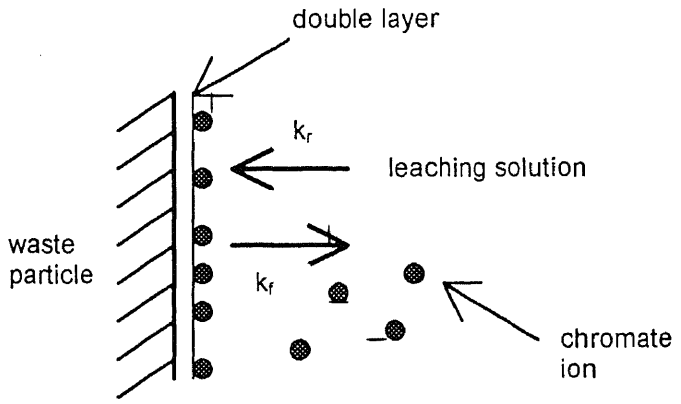

Figure 4.6 Mass transfer of Cr(VI) during the leaching.

We need an initial condition, before we integrate equation 4.3. We would like to assume that at t = 0, q = 0. If we take a look at Figure 4.5, we notice that none of the curves start at q = 0 when t = 0. It looks like every leaching process consists of two steps.

1. A fast dissolution step that appears in a few minutes (probably an ordinary dissolution). The amount leached out by this first step is given by the q value at t = 0.
2. A second step that is spread out over several days and that is enhanced by the presence of anions in the solution (probably dominated by desorption and ion-exchange).

As an attempt to divide those two steps, we subtracted the q value at t = 0 from every experimental q value that is used to construct the curves in Figure 4.5. By doing so, we exclude the first leaching step and we restrict the fitting, using equation 4.3, to the second step. The q values at t = 0 for each of the curves are given in Table 4.11.

Table 4.11 q value at t = 0.

leaching solution	q at t = 0 (mg/g waste)
pure deionized water	0.88
0.1 M NaCl solution	1.71
0.1 M Na_2SO_4 solution	2.09
0.1 M Na_3PO_4 solution	0.87

Now we can introduce the initial condition q = 0 at t = 0. After integration, equation 4.3 becomes:

$$q = k_f q_\infty /(k_r + k_f)\{1 - \exp(- (k_r + k_f)t\} \qquad (4.4)$$

We assume that the reverse reaction is insignificant compared to the forward reaction or: $k_r <<< k_f$, so equation 4.4 can be simplified as:

$$q = q_\infty \{1-\exp(- k_f t)\} \qquad (4.5)$$

This equation was used to fit the four experimental curves shown in Figure 4.5. To perform the fitting, q was plotted as a function of (1- exp(- $k_f t$)) and a best linear fit was obtained (Figures 4.7 to 4.10). From these Figures, we obtained the values of k_f and q_∞ (Table 4.12).

Table 4.12 Fitted values of k_f and q_∞.

leaching solution	k_f (1/min.)	q_∞ (mg/g waste)
pure deionized water	1/30	0.63
0.1 M NaCl solution	1/1100	2.62
0.1 M Na_2SO_4 solution	1/1500	5.61
0.1 M Na_3PO_4 solution	1/2500	5.20

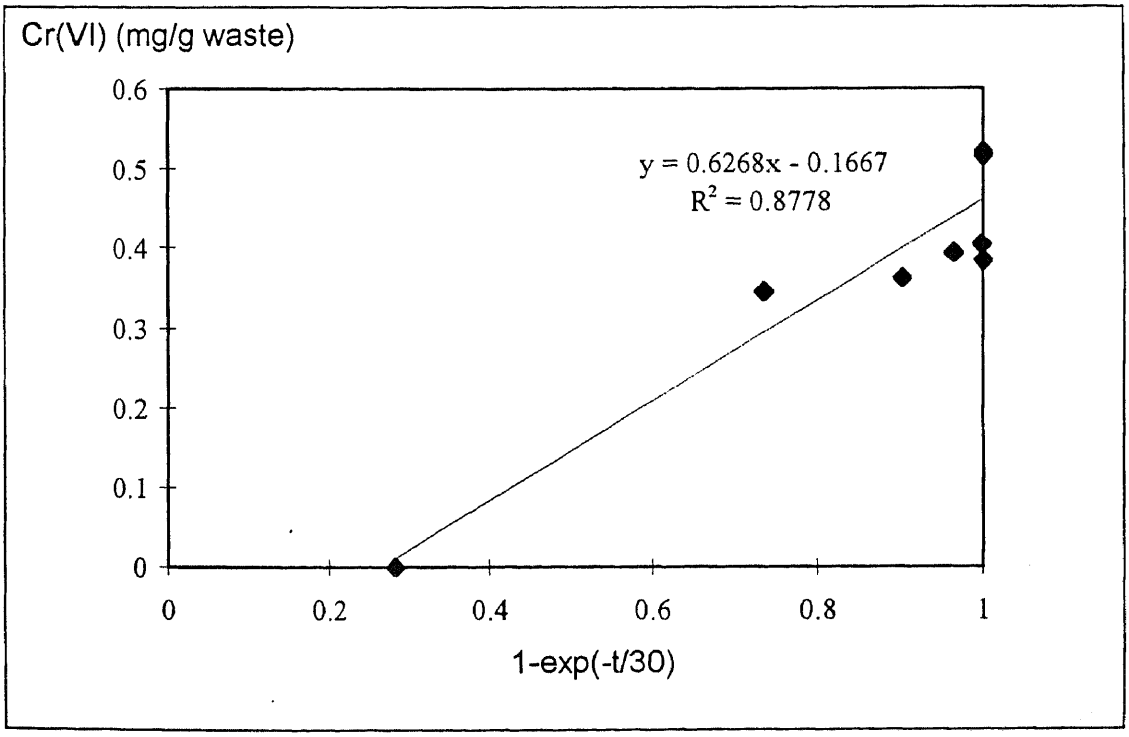

Figure 4.7 Best fitting when water was used as leaching solution.

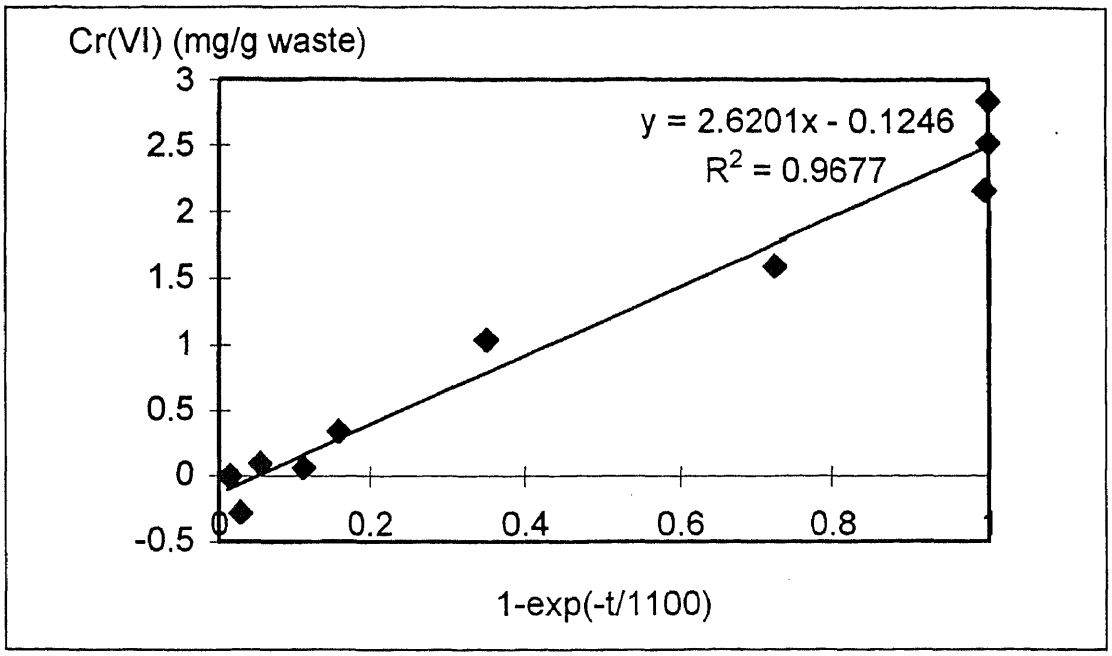

Figure 4.8 Best fitting when 0.1 M NaCl was dissolved in the leaching solution.

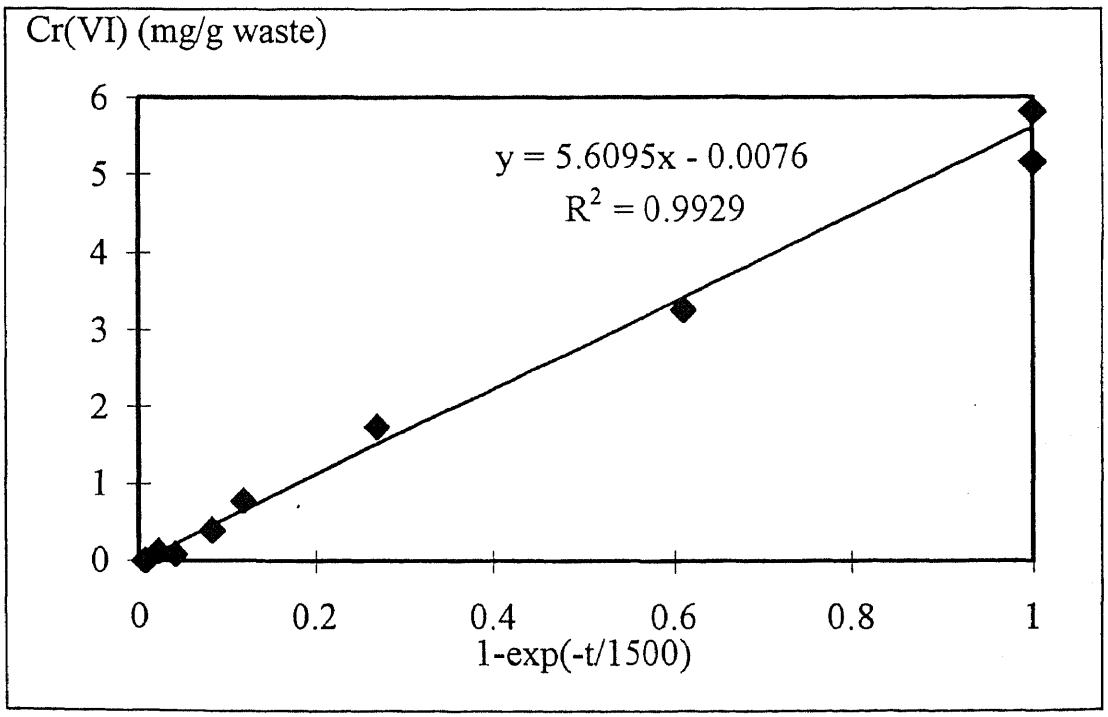

Figure 4.9 Best fitting when 0.1 M Na_2SO_4 was dissolved in the leaching solution.

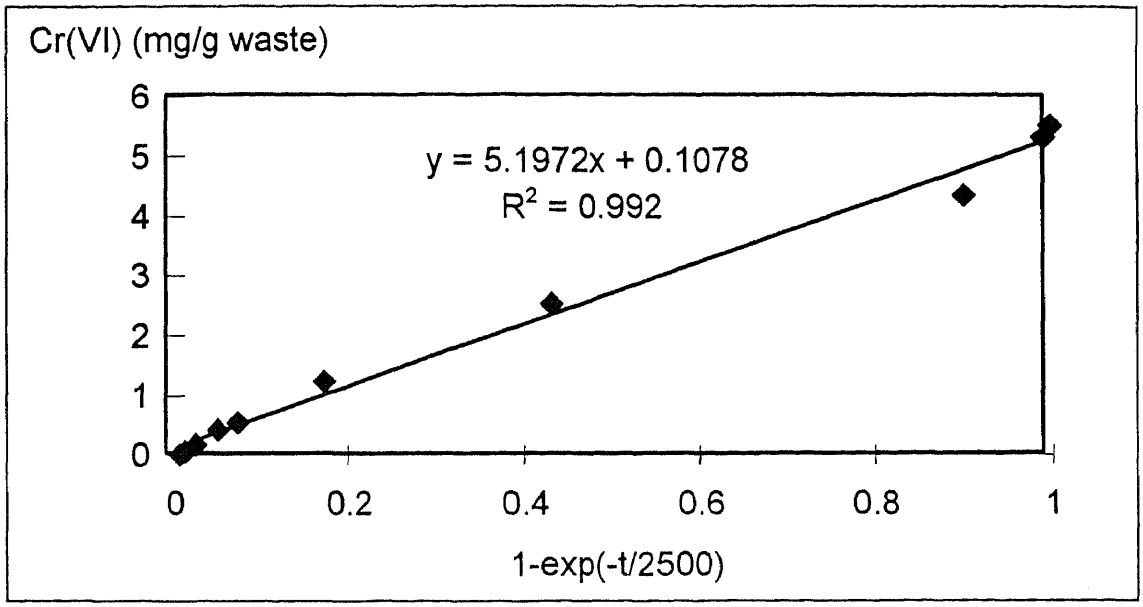

Figure 4.10 Best fitting when 0.1 M Na_3PO_4 was dissolved in the leaching solution.

The rate of dissolution is the highest for pure water and the dissolution occurs only in a short time after exposure. For the salt solutions the dissolution rate becomes slower when the size of the salt anion becomes bigger. This can be caused by a restriction of the transportation of the salt anions through the complex microstructure of the waste material. Based on these results, mass transportation seems to be the rate determining factor.

The maximum Cr(VI) removed in the second step (q_∞) was compared to values obtained in the literature, where a similar type of adsorbents were used. Reference 4 describes the adsorption of chromate on goethite. The goethite is environmentally relevant and represents a larger group of adsorbents. From a Langmuirian adsorption isotherm in Reference 4, it was found that a maximum of 3.2×10^{-6} mol/m^2 can be adsorbed on the adsorbent. For our waste, the specific

surface is around 20 m^2/g (Ref. 12). So, 6.4 x 10^{-5} mol/g waste or 3.3 mg/g waste is the maximum amount of chromate, that may be adsorbed on the waste. Note that this number is only valid for monolayer adsorption, which is one of the conditions for Langmuirian adsorption. We compared this number with the maximum q_∞, obtained in the case of 0.1 M Na_2SO_4 leaching (q_∞ = 5.61 mg/g waste). This is higher than the monolayer coverage obtained from Reference 2. Therefore, it can be concluded that we are dealing with a multiple layer adsorption. In reality, the distribution of chromium in the waste is very complex as evidenced by our SEM-EDS elemental mapping (Chapter 3, Section 3.3.4).

It should be noted that the q_∞ in Table 4.12 is the maximum Cr(VI) removal from the second step of the leaching. To compare the total maximum Cr(VI) removal from the fitting (q_∞^*) with the experimental values q_∞^{exp} (Table 4.10), we have to add the values of Cr(VI) removed in the first step, (Table 4.11). Table 4.13 shows the comparison between q_∞^* and the experimental values from Table 4.10.

Table 4.13 Comparison of q_∞^* and q_∞^{exp}.

leaching solution	q_∞^* (mg/g waste)	q_∞^{exp} (mg/g waste)
pure deionized water	1.51	1.40
0.1 M NaCl solution	4.33	4.55
0.1 M Na_2SO_4 solution	7.70	7.92
0.1 M Na_3PO_4 solution	6.07	6.38

4.3.6 Proposal for Cr(VI) Removal from the Waste

The highest removal efficiency (q_∞^{exp} = 7.92 mg/g waste) was obtained in the kinetics experiment with the 0.1 M Na_2SO_4 leaching solution. However, it takes several days to reach the maximum removal efficiency. Therefore, we tried to design a faster method to attain the same removal efficiency (7.92 mg/g waste). Our process consisted of three steps:

1. We added 500 ml of 0.1 M Na_2SO_4 leaching solution to our waste, stirred it thoroughly and let it stay for a few hours. We then separated the waste and solution by filtration. The Na_2SO_4 was chosen because of its high removal efficiency, as described earlier.
2. The recovered waste from the first step is added to a new 500 ml of 0.1 M Na_2SO_4 leaching solution and the same treatment as in step 1 was repeated.
3. The recovered waste from the second step is added to 500 ml of 0.2 M $NH_4F.HF$ leaching solution and again the waste is separated from the solution by filtration after a few hours. We choose $NH_4F.HF$ in this last step because it has a high removal efficiency and it has the property to seal the waste from the environment (Ref. 3).

The following Cr(VI) removal was obtained in each step for the three experiments performed (Table 4.14).

Table 4.14 Cr(VI) removed in each step of the proposed treatment [mg/g waste].

	experiment 1	experiment 2	experiment 3
step 1	4.07	5.20	4.99
step 2	0.54	0.405	0.69
step 3	3.135	2.00	1.62
total removal	7.75	7.605	7.30

In the conducted treatment experiments, the total Cr(VI) removal does not equal q_{∞}^{exp} = 7.92 (mg/g waste). Complementary experiments (1', 2' , and 3') were performed to see if their is still Cr(VI) leached out in pure water solutions at pH 7. The following Cr(VI) concentrations were measured in the leachate solutions(Table 4.15):

Table 4.15 Cr(VI) leached out after treatment [mg/g waste].

experiment 1'	experiment 2'	experiment 3'
0.065	0.077	0.048

Once the waste is treated with the proposed technique, only a negligible amount of Cr(VI) will be released if the waste is immersed in water.

4.4 Conclusions

By performing consistent and systematic experiments, we were able to make the following conclusions about the behavior of the chromate in the waste:

1. Pure water has the ability to dissolve some of the chromate, but could not achieve its effective removal. When salts are added to the water, the removal

of Cr(VI) from the waste significantly increases. We were able to remove 39 % of the total chromium in the waste as chromate, - almost the same percentage of Cr(VI) as determined by XPS analysis.

2. It seems that the leaching of Cr(VI) can be divided into two steps: The first step where an immediate dissolution takes place, and the second step where a slow desorption occurs as part of an ion-exchange at accessible surface pores.
3. A new treatment technique is proposed to remove the majority of accessible chromate with salt solutions. Here a sequence of leaching/washing with sulfate and bifluoride was used.

CHAPTER 5

OXIDATIVE DISSOLUTION OF CR(III) TO CR(VI)

5.1 Background and Objectives

In Chapter 4, we described how Cr(VI) could be leached out or removed from the chromium residue waste. From advanced characterization results, described in Chapter 3, we also know that there is a considerable amount of Cr(III) in the waste. We can consider that all the Cr(III) in the highly basic waste will be present as $Cr(OH)_3.nH_2O$ (Ref.8). Due to its low solubility, $Cr(OH)_3.nH_2O$ does not leach out easily into the aqueous environment (Ref. 12). In order to remove all the Cr(III) from the studied waste by extraction as is conducted by others, it is necessary to use hot acids at high concentrations (pH less than 1). Under such conditions, other metals (Ca, Fe, Al, Mg) are also extracted; the waste looses up to 50 % of its original weight (Ref. 7). Therefore, most of the added acid is used to dissolve the waste matrix. This makes this approach impractical. We have studied the process of oxidative dissolution to leach and remove Cr(III) from the waste. An account of this study is given in this chapter.

Oxidative dissolution is a process where insoluble Cr(III) species are oxidized to the more soluble Cr(VI) form. The latter is readily leached out into the aqueous environment. In our case, solid $Cr(OH)_3.nH_2O$ in the waste residue is oxidized to Cr(VI), (CrO_4^{2-}), which can be leached out easily by aqueous solutions.

In this chapter we have studied the oxidative dissolution process using different oxidants at various pH conditions. Our objective was to define a mechanism for Cr(III) transformation to Cr(VI) and the leaching of the latter into the environment. Based on our experimental results, predictions can be made regarding the above important process. Cr(III) is not, by itself, considered to be an important environmental issue because of its low solubility and low mobility in the natural environment. Nevertheless, as we will show in this chapter, it is possible to oxidize Cr(III) to Cr(VI) and to leach it out into the environment. Also in this chapter we will assess the conditions and rate for the conversion and leaching processes.

5.2 Materials and Methods

5.2.1 Materials

All the experiments (except those involving H_2O_2) were conducted with chromium waste samples after they were treated with the technique outlined in Chapter 4 - i.e., two consecutive leaching steps with 0.1 M Na_2SO_4 solutions and one leaching with an 0.2 M $NH_4F.HF$ solution. Based on our XPS results, most of the "accessible" Cr(VI) is removed from the waste by the application of this treatment method. The chromium detected in the solution samples during the oxidative dissolution can therefore be considered to be contributed by Cr(III) species that are oxidized to soluble chromate.

5.2.2 Methods and Experimental Procedures

We studied the influence of the concentration of added oxidants on the dissolution of the Cr(III) from chromium waste residue. We have employed different oxidants with diverse oxidation properties (H_2O_2, $KBrO_3$, $KMnO_4$ and Ce(IV)). H_2O_2 was applied to the as-received waste residue to determine if H_2O_2 can convert Cr(III) to Cr(VI). This conversion was verified by XPS analysis to determine Cr(III)/Cr(VI) after exposure to H_2O_2. The H_2O_2 solutions were added at once, to the waste. After the reaction was completed, the treated waste was dried and used for XPS characterization.

For the other oxidants, we added the concentrated oxidant solutions stepwise, by means of a burette, to keep the temperature constant around room temperature. After each addition of the solution we restirred the content of the beaker and waited for particles to settle. The actual oxidant concentration was calculated and a sample of the leachate was taken for AA analysis. The oxidant was added to several beakers at the same time. The content of each of this beakers was held at a different constant pH condition. By following the above procedure, we were able to study the effect of oxidant type and concentration (and therefore the influence of Eh) on the conversion (Cr(III) to Cr(VI)) and the leaching into the solution at several pH conditions. Adjusting of the pH was achieved by adding small amounts of acid (H_2SO_4) or base (NaOH) to the leaching medium.

5.3 Results and Discussion

The following pH values: 3, 5, 7, 9, 10, and 11.5 were used in our oxidative dissolution experiments. We have avoided pH conditions below 3 because the waste material significantly dissolves in acids (Figure 5.1).

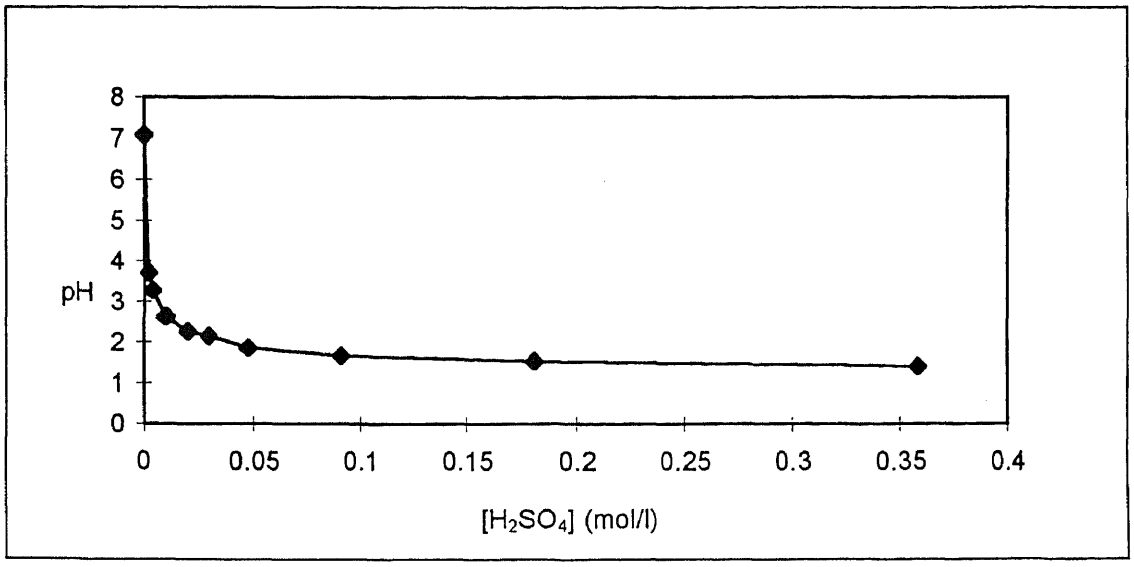

Figure 5.1 Acid consumption by waste - pH versus amount of acid added.

5.3.1 Thermodynamic Consideration of Oxidative Dissolution

To specify the reactions that took place during the oxidative dissolution at different pH values, we refer to the Pourbaix diagram for chromium (Ref. 8) (Figure 5.2).

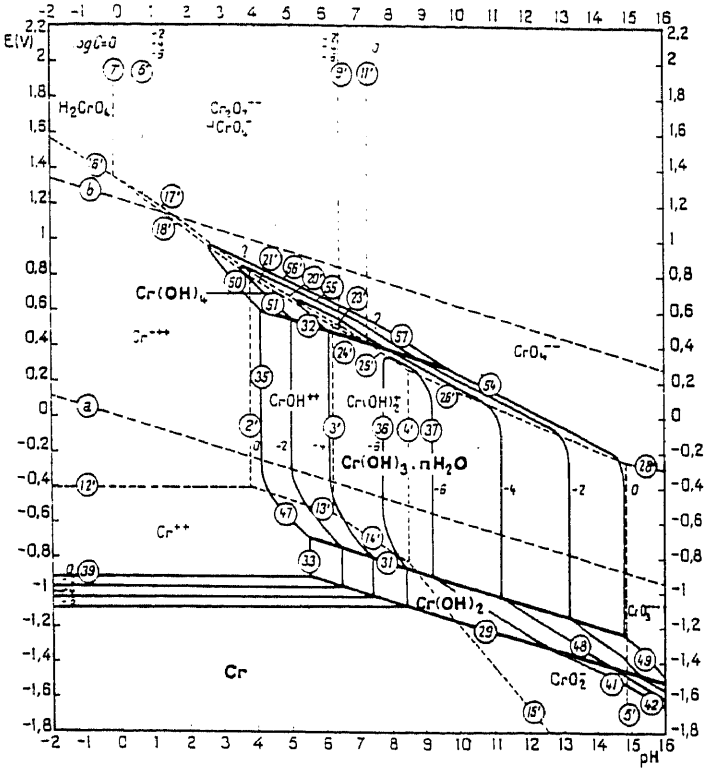

Figure 5.2 Potential-pH diagram for the system chromium-water, at 25 ^{0} C.

The reaction that is responsible for the oxidation of $Cr(OH)_3.nH_2O$ to CrO_4^{2-} is given by equation 5.1 for pH 10 and 11.5. At pH 9, the oxidation to CrO_4^{2-} proceeds via the formation of $Cr(OH)_4$ (equation 5.2). $HCrO_4^-$ will be formed through the formation of $Cr(OH)_4$ at pH 5 and 7 (equation 5.3). At pH 3, $Cr(OH)_3.nH_2O$ is dissolved as Cr^{3+} before the oxidation to $HCrO_4^-$ takes place.

$$2Cr(OH)_3.nH_2O + 2H_2O \leftrightarrow 2CrO_4^{2-} + 10\,H^+ + 2n\,H_2O + 6e^- \quad (5.1)$$

$$CrO_2 + 2H_2O \leftrightarrow CrO_4^{2-} + 4H^+ + 2e^- \quad (5.2)$$

$$CrO_2 + 2H_2O \leftrightarrow HCrO_4^- + 3H^+ + 2e \quad (5.3)$$

The Nernst equations associated with these oxidation reactions are given by equations 5.4, 5.5, and 5.6 respectively. (Ref. 8).

$$E_0 = 1.244 - 0.0985pH + 0.0197\log(CrO_4^{2-}) \quad (5.4)$$

$$E_0 = 1.437 - 0.1182pH + 0.0295\log(CrO_4^{2-}) \quad (5.5)$$

$$E_0 = 1.246 - 0.0886pH + 0.0295\log(CrO_4^{2-}) \quad (5.6)$$

These equations are used to construct lines 54, 57, and 55 respectively in the potential-pH diagram (Pourbaix diagram) for chromium-water systems (Figure 5.2). The lines were constructed for different concentrations of CrO_4^{2-}, respectively 1, 10^{-2}, 10^{-4}, 10^{-6} mol/l. The highest chromate concentration that can be attained in our experiments can be calculated by assuming total dissolution of the remaining chromium. During our pretreatment, between 36 and 38 % of the total chromium content is removed from the waste. 64 % of the total chromium will remain in the waste material used in these experiments. Dissolution of all the remaining chromium would result in a concentration of 0.0025 mol/l (64 % of total chromium (= 2.03 % of 5 g. of waste), volume solution = 0.5 l.). If we use 0.0025 mol/l as the CrO_4^{2-} concentration in equations 5.4-5.6, we find the following relationships between Eh and pH (equation 5.7 for pH 10 and 11.5, equation 5.8 for pH 9, and equation 5.9 for pH 5 and 7).

$$E_0 = 1.193 - 0.0985pH \quad (5.7)$$

$$E_0 = 1.360 - 0.1182pH \quad (5.8)$$

$$E_0 = 1.169 - 0.0886pH \quad (5.9)$$

The physical meaning of these lines is the following: If for a certain pH, the Eh is higher than the one calculated with one of the above equations (5.7-5.9), more than 0.0025 mol/l of Cr(III) can be dissolved by oxidation in the solution. If we stay above the lines described by equations 5.7-5.9 in the Pourbaix diagram (Figure 5.2), we should then be able to dissolve all the Cr(III) through oxidation in soluble Cr(VI) (if all the Cr(III) is accessible). Based on equations 5.7-5.9 some Eh values were calculated for the different pH values used in the experiments (Table 5.1).

Table 5.1 Eh versus pH determined by equation 5.7-5.9 - conditions for Cr(III) → Cr(VI) conversion.

pH	5	7	9	10	11.5
Eh (V)	0.726	0.549	0.296	0.208	0.060

In order to confirm if we will work under oxidizing conditions during all of our experiments, we have to compare the values of Table 5.1 with the lowest oxidation potentials measured in our experiments. The lowest oxidation potentials in our experiments are those measured when no oxidant is used (Table 5.2).

Table 5.2 Measured Eh values of the leachate after pretreatment without oxidant.

pH	5	7	9	10	11.5
Eh (V)	0.729	0.553	0.408	0.304	0.232

If we compare these Eh values to those given in Table 5.1, we see that the lowest measured Eh values are higher than those required for oxidation of all the remaining chromium in the waste. This means that the aqueous environment at the site, even without the addition of any reagent, favors the oxidative dissolution of the Cr(III) in the waste. We should conclude that the oxidizing conditions prevails during all the experiments, and that we do not have to consider the reduction of the Cr(VI) species to Cr(III) species during our experiments. All the chromium detected in the leachate will be Cr(VI) species. We plotted Eh values versus pH for solutions added to the waste with and without oxidant (Figure 5.3).

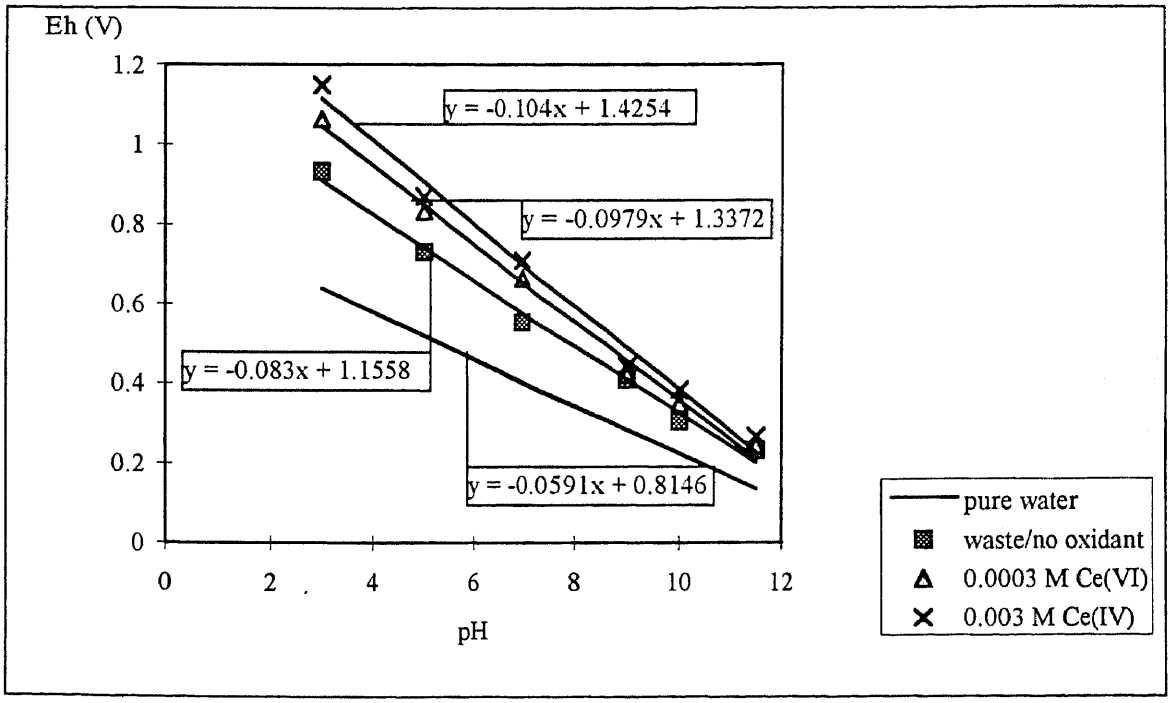

Figure 5.3 Eh versus pH of leachate with and without oxidant.

When water with oxidant is added to the waste the negative slope increases with the amount of oxidant added. Therefore, we can conclude that the slope gets steeper due to increase in the concentration of oxidized species in the solution. If the waste is added to pure water, without oxidant, the slope of the Eh/pH relationship becomes steeper than in the case of pure water without waste. As we pointed out earlier, the Eh versus pH follows a straight line with a slope of -0.0591 V/pH for pure water without waste. With the waste the slope becomes -0.083 V/pH. When the waste is immersed in pure water oxidizing species like Fe(III), Cr(VI),... are dissolved in the leaching solution and result in a steeper slope of the Eh/pH relationship.

5.3.2 Conversion of Cr(III) to CR(VI) by Oxidants - XPS Analysis of Waste Samples after Treatment with Oxidative Dissolution

To determinate the conversion of Cr(III) to Cr(VI), we treated the as received waste samples (20 g.) with various concentrations of H_2O_2 solutions (50 ml.). The resulting treated solid was analyzed by XPS to determine the ratio of valence states as a function of H_2O_2 concentration (Table 5.3). Based on the values of Table 5.3, we calculated the Cr(III)/Cr(VI) ratio. This ratio is plotted versus $[H_2O_2]$ in Figure 5.4.

Table 5.3 Cr(III)/Cr(VI) determined by XPS for different concentrations of added H_2O_2.

$[H_2O_2]$ (mol/l)	Cr(IV) % of total Cr on surface	Cr(III) % of total Cr on surface
0	47	53
0.025	59	41
0.127	62	38
0.255	68	32
1.273	67	33
2.545	69	31
5.090	73	27
7.635	74	26

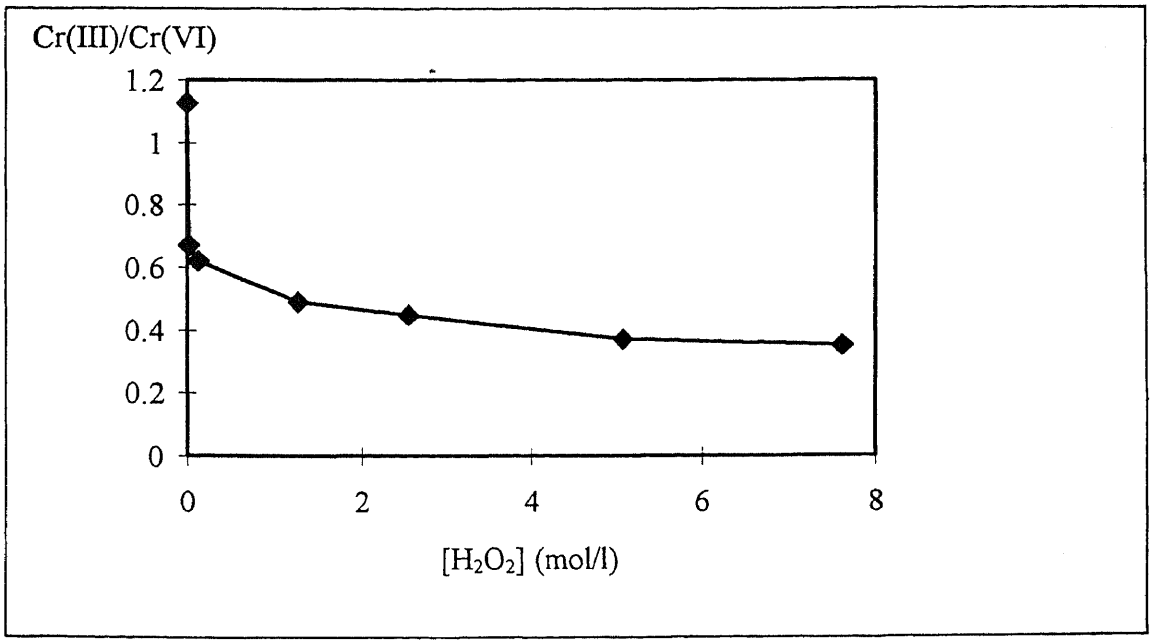

Figure 5.4 $[H_2O_2]$ versus Cr(III)/Cr(VI) on the surface of the waste particles.

The results of Table 5.3 and Figure 5.4 show that H_2O_2 produces a significant Cr(III) $\rightarrow$ Cr(VI) conversion by reaction at the interface of the waste particles. We could decrease Cr(III) by a factor of 2. For high concentrations of added oxidant,

the Cr(III)/Cr(VI) ratio reaches a plateau value of 0.35. We could not do further oxidation of Cr(III) to Cr(VI) beyond this limit, possibly because of mass transport restrictions. The remaining Cr(III) is believed to be inaccessible to H_2O_2 solution. This experiment is an excellent evidence of the conversion of Cr(III) to Cr(VI) in the waste.

5.3.3 Influence of Oxidant Type and Concentration and the Effect of pH Condition on Oxidative Dissolution

The influence of oxidant concentration was studied for different oxidants: $KBrO_3$, $KMnO_4$ and Ce(IV). By changing the concentration of the oxidants, the Eh value of the leaching solution was changed. During these experiments the pH was held constant. We were able to study the influence of Eh and pH on the oxidative dissolution of Cr(III). At the end of this section a three dimensional graph was constructed, where we plotted the Cr(III) that was converted to Cr(VI) and dissolved in the leachate as a function of pH and Eh.

The conditions under which the experiments are performed are given in Table 5.4.

Table 5.4 Description of the experiments.

Oxidant	maximal conc. of oxidant (mol/l)	pH	amount of waste (g.)	volume of leachate (ml.)
$KBrO_3$	0.08	3,5	5	500
$KMnO_4$	0.08	3,5,7	5	500
Ce(IV)	0.003	3,5,7,9,10,11.5	5	500

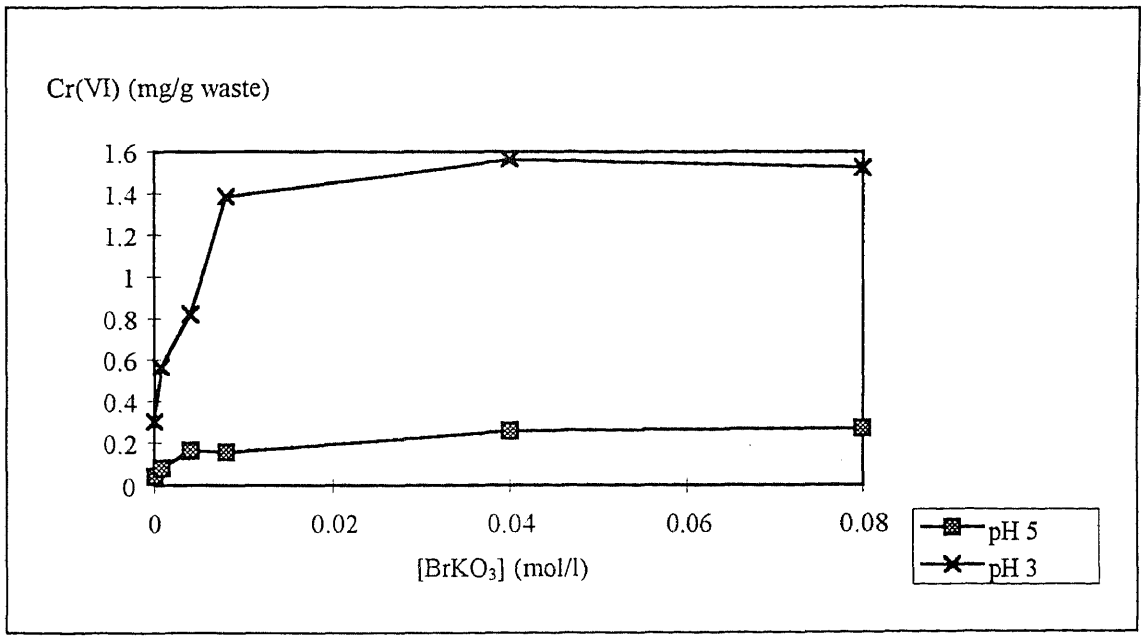

Figure 5.5 Oxidative dissolution with $KBrO_3$.

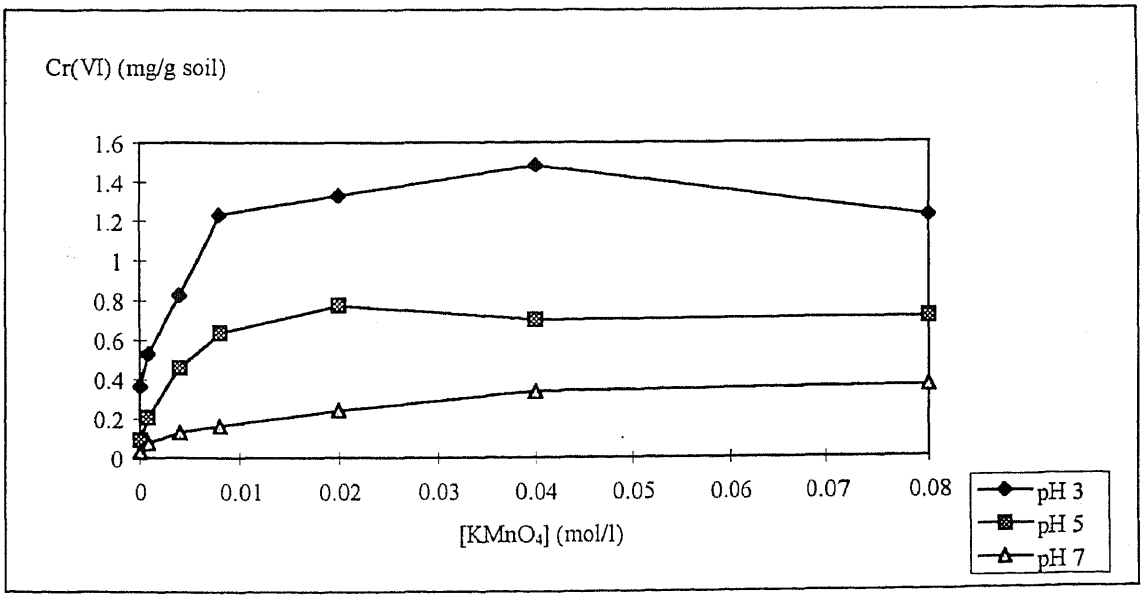

Figure 5.6 Oxidative dissolution with $KMnO_4$.

Table 5.5 Oxidation potentials recorded during the experiments (mV).

	$KBrO_3$		$KMnO_4$				Ce (IV)					
conc.	pH 3	pH 5	pH 3	pH 5	pH 7	conc.	pH 3	pH 5	pH 7	pH 9	pH 10	pH 11.5
0.0008	923	776	1166	1028	872	0.00006	991	825	599	440	343	243
0.004	964	826	1205	1091	881	0.0003	1062	832	663	421	349	243
0.008	993	832	+1200*	1102	909	0.0006	1075	882	697	458	351	252
0.02			+1200*	1105	932	0.0015	1122	916	698	399	338	247
0.04	1027	889	+1200*	1074	935	0.003	1149	869	709	442	383	267
0.08	1035	881	+1200*	1106	941							

(*) The exact Eh value couldn't be measured because it was out of the range of the ORP meter.

in the solution at pH 3 is much higher than at higher pH conditons (5,7, ...). As discussed earlier, this can be explained by the fact that at pH 3, Cr(III) is dissolved in the leachate. This Cr^{3+} will then be oxidized to $HCrO_4^-$ in the solution because of the high oxidation potential. At higher pH conditions, the dissolution of Cr(III) is limited. At such higher pH, Cr(III) must be oxidized to Cr(VI) in the solid state of the waste, before it can be leached as CrO_4^{2-} or $HCrO_4^-$ in the solution. There are two possible reasons why only small amounts of Cr(III) are leached in the solution by means of oxidative dissolution at higher pH compared to pH 3.

1. The oxidation of the Cr(III) in the solid state happens through the formation of surface complexes at the interface between waste particles and solution (Ref. 10,11). This process is more complicated than a simple redox reaction that is known in solution chemistry.
2. For reactions that occur at the interface of particulates with complex microstructure (and pore structure), physical accessibility to reagent has major effect on mass transfer and leaching.

The experiments with $KBrO_3$ and $KMnO_4$ are compared in Figure 5.8, because they were performed with the same concentrations.

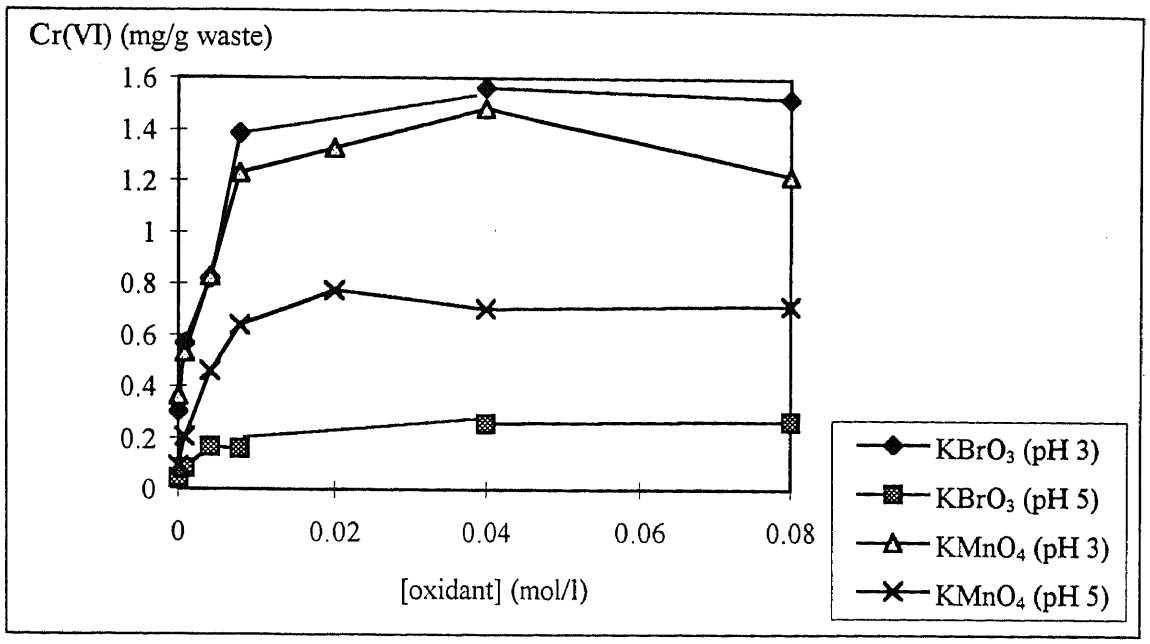

Figure 5.8 Comparison between the use of $KBrO_3$ and $KMnO_4$.

The highest oxidation potentials are obtained with $KMnO_4$. The oxidation potential does not control the solubility of Cr(III) in case of Cr^{3+} dissolution at pH 3. The experiments with $KBrO_3$ and $KMnO_4$ at pH 3 show that the same amount of Cr(III) is released in the leachate (1.5 mg/ g waste or 6 % of the total chromium in the waste). However, at pH 5, we notice a significant difference between $KBrO_3$ and $KMnO_4$ results. Here the amount of Cr(III) dissolved with $KMnO_4$ is around three times higher than with $KBrO_3$. At pH 5, we are dealing with interfacial oxidative dissolution _ oxidant reacts with the surface to convert Cr(III) to Cr(VI) and the latter is then released into the solution. This interfacial reaction is faster with $KMnO_4$ than with $KBrO_3$.

The experiments done with Ce(IV) show a lower amount of Cr(III) dissolved in the leachate than the experiments with $KBrO_3$ and $KMnO_4$. This is because of two reasons:

1. The concentrations used in the experiment with Ce(IV) were a lot smaller due to the solubility limitations of the Ce(IV) salt - $(Ce(NH_4)_2(NO_3)_6$.
2. Ce(IV) has the tendency to form complexes with sulfate, that was added to the solution as H_2SO_4 to keep the pH low after the alkaline waste was added.

Based on the experiments with $KMnO_4$ and Ce(IV) that were conducted at different pH values, we were able to construct the following three dimensional diagrams (Figure 5.9 and 5.10).

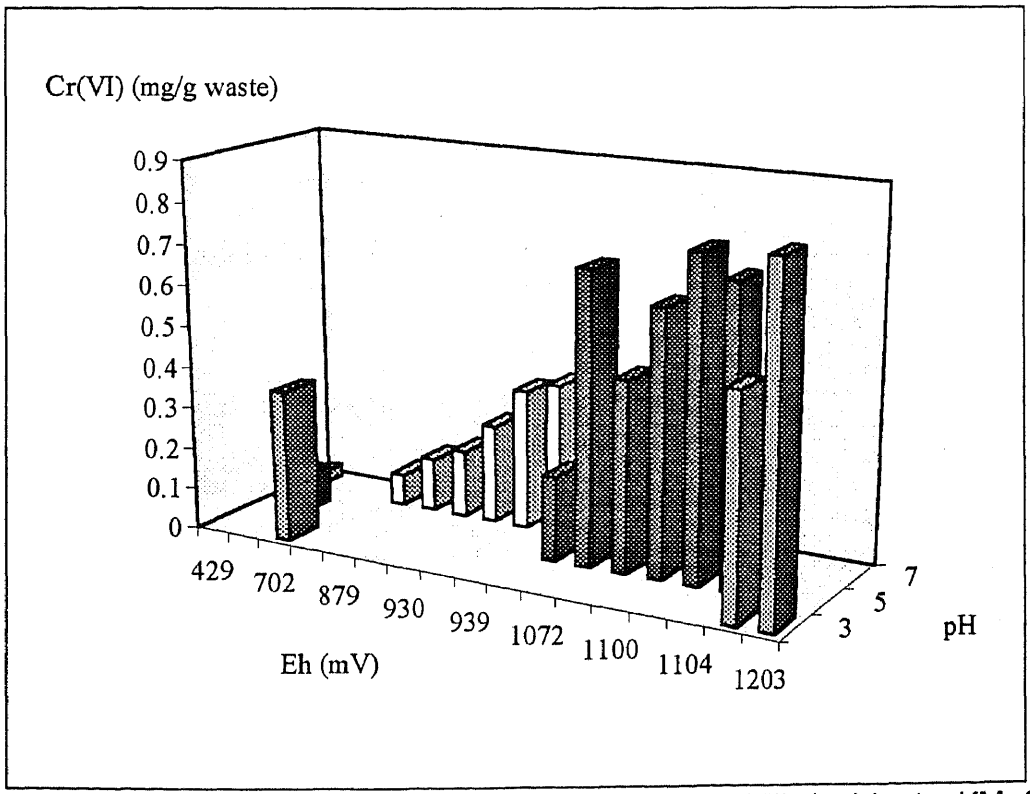

Figure 5.9 Cr(III) dissolved as Cr(VI) versus pH and Eh (oxidant = $KMnO_4$).

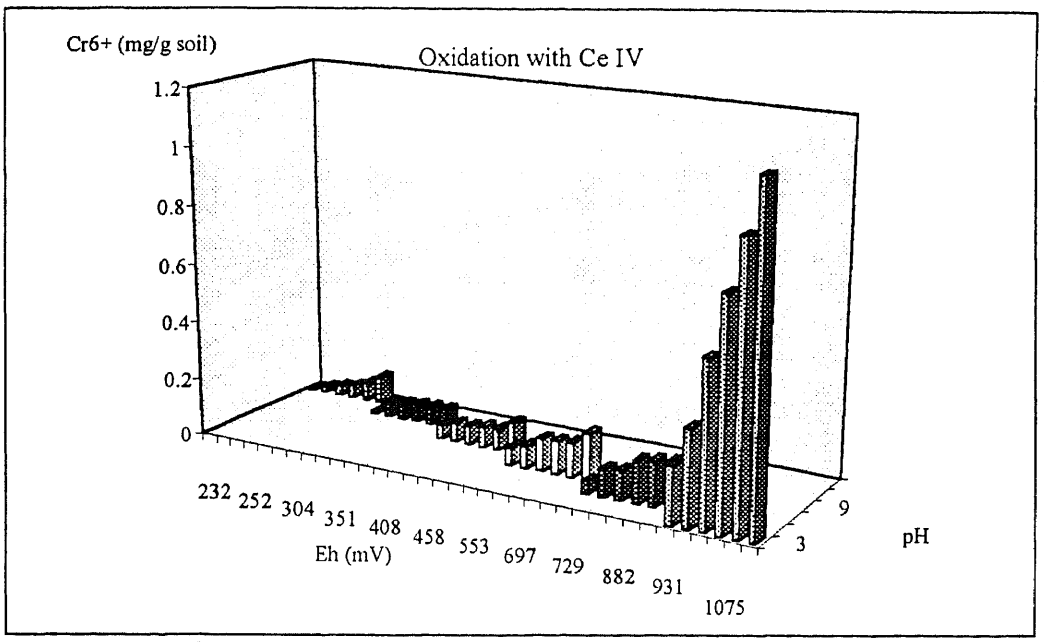

Figure 5.10 Cr(III) dissolved as Cr(VI) versus pH and Eh (oxidant = Ce(IV)).

In both cases (with $KMnO_4$ and Ce(IV) as oxidant) we can conclude that the best leachability of Cr(III) from the waste is attained under high Eh and low pH conditions. This is consistent with acid dissolution followed by oxidation in the aqueous phase. This may be the most important mechanism for this process in the environment.

5.3.4 Kinetics of Dissolution of Cr(III) at Low pH

We choose $KMnO_4$ as oxidant for our kinetics experiment. Again we conducted our experiment at different constant pH conditions (3, 5, and 7). We added 500 ml. of a 0.08 M $KMnO_4$ solution to 5 g. of pretreated chromium waste. Our experimental results are plotted in Figure 5.11.

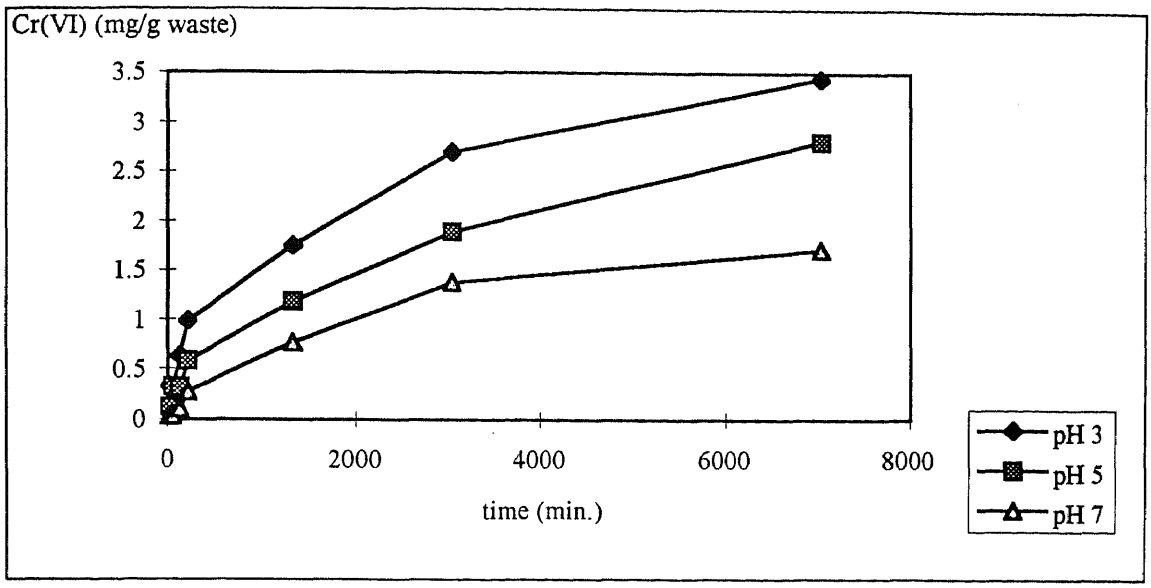

Figure 5.11 Kinetics experiment with $KMnO_4$.

In the previous section, we found that only a maximum of 6 % of the total chromium can be removed from the waste by dissolution, while there is still 60 % of the total chromium present in the waste after the pretreatment (most of it as Cr(III). So there is a lot of Cr(III) that cannot be removed by dissolution probably because of mass transport restrictions. Based on this hypothesis, the experimental data was fitted with the parabolic rate law (equation 5.10), which is a rate equation corresponding to a transport-controlled reaction - diffusion limited case (Ref. 11).

$$dC/dt = k_p t^{-1/2} \qquad (5.10)$$

where,

k_p = reaction rate constant [M $min^{-1/2}$],

t = time [min.], and

C = concentration in the solution [mg/g waste](Cr(VI) in our case).

By integration, the concentration C increases with square root of time (equation 5.11)

$$C = C_0 + 2k_p t^{1/2} \qquad (5.11)$$

The experimental curves were fitted with equation 5.11 and the best fits are shown in Figures 5.12, 5.13, and 5.14.

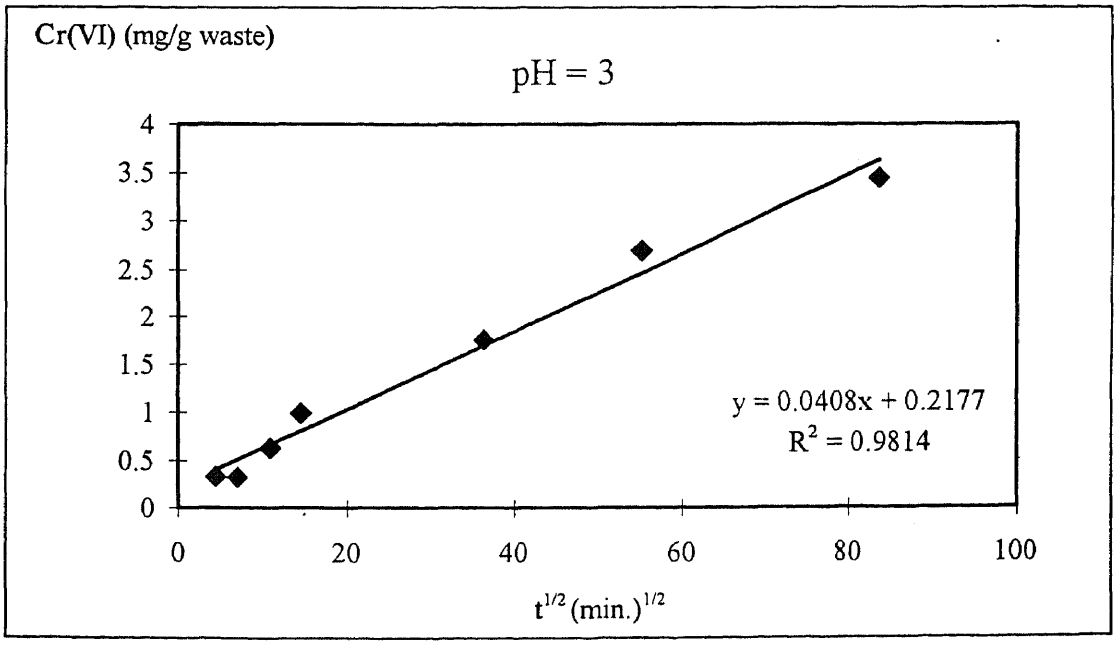

Figure 5.12 Best fit of the kinetics experiment (pH = 3).

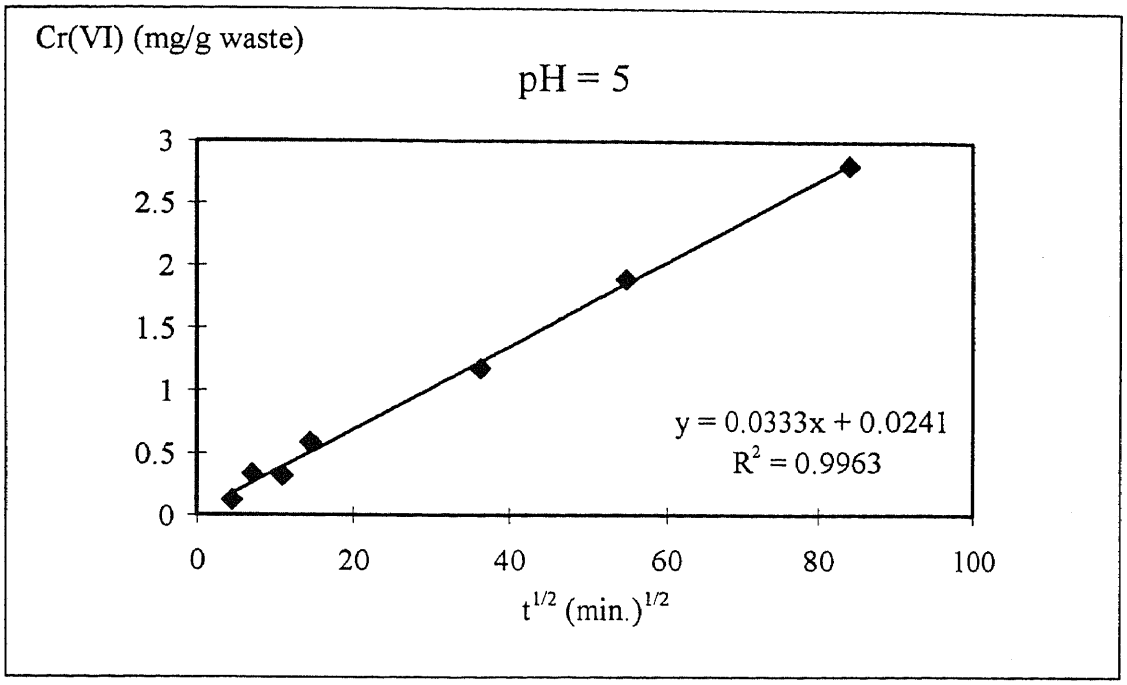

Figure 5.13 Best fit of the kinetics experiment (pH = 5).

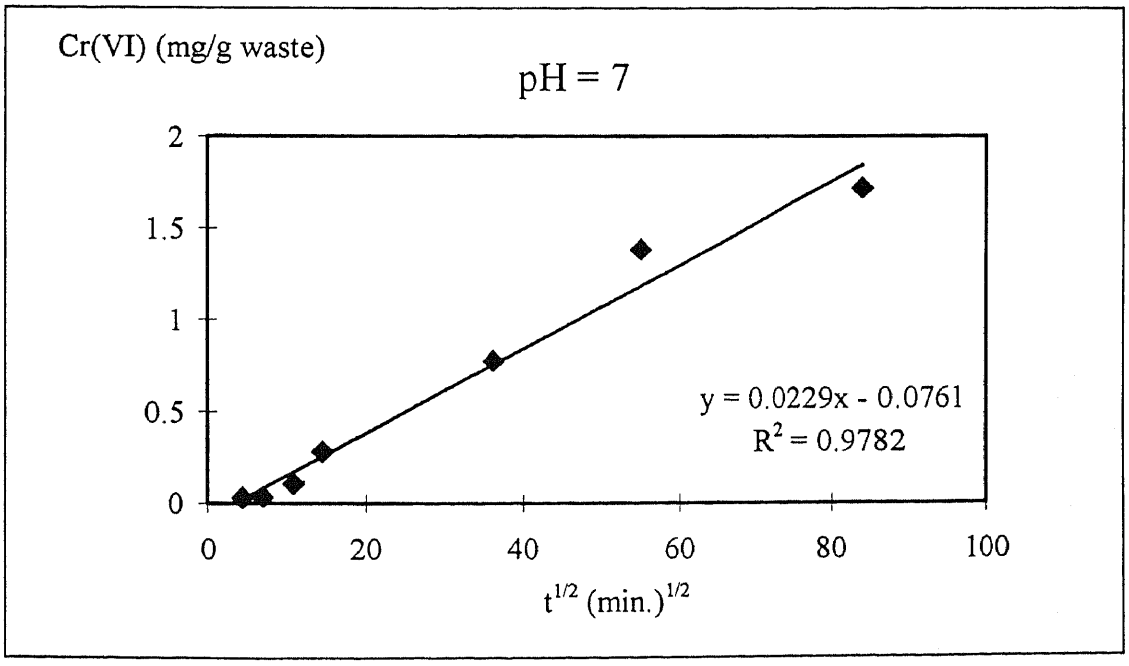

Figure 5.14 Best fit of the kinetics experiment (pH = 7).

Based on the linear equations of the best fittings given in Figure 5.12 - 5.14, we obtained the following values for the reaction rate constant k_p and the concentration C_0 at t = 0 (Table 5.6):

Table 5.6 Reaction rate constants for transport controlled dissolution of Cr(III).

pH	3	5	7
k_p [M $min^{-1/2}$]	0.020	0.017	0.012
C_0 [mg/g waste]	0.218	0.024	0.076

The higher the pH, the lower the value of k_p and the slower the reaction will occur. The rate constant at pH 7 is still significant, and should be considered for the case of Cr(III) in landfills. Only at pH 3 we find a significant value of C_0. At low pH, the highly accessible Cr(III) is leached by immediate dissolution, which explains a C_0 different from 0. At higher pH we do not deal with straight dissolution and therefore, the measured C_0 values are insignificant at pH 5 and 7.

5.4 Conclusions

We deal with a combination of a straight dissolution of $Cr(OH)_3.nH_2O$ to Cr^{3+} followed by an oxidation to $HCrO_4^-$ in the leaching solution when the pH is low (pH 3). An oxidative dissolution occurs for higher pH, where the oxidation to chromate occurs at the interface between waste particles and the leaching solution. The oxidation is then followed by the dissolution of the chromate in the leaching solution. The amounts of Cr(III) that are leached out stay very low

when the oxidative dissolution occurs _ mostly at high pH. The maximum of Cr(III) removed under these conditions was 0.77 mg/g waste or 3.8 % of the total chromium (pH 5 with 0.08 M $KMnO_4$). If we want to check if Cr(III) can be leached in the environment, we should be more concerned about the acid dissolution and oxidation at low pH conditions.

Based on kinetics experiments, we were able to determine that the leaching of Cr(III) as Cr(VI) follows a transport-controlled rate equation. The mass transport restriction seems to be the significant factor in determining leaching rates of Cr(III) under oxidative conditions.

CHAPTER 6

CONCLUSIONS

By means of advanced spectroscopic characterization techniques, we were able to construct a detailed picture about the chromium waste residue. Our chromium waste sample consists of a complex mixture of crystalline and amorphous phases. Most of the chromium is present on the surface of the waste particles as Cr(III), ($Cr(OH)_3.nH_2O$), and as Cr(VI), (CrO_4^{2-}). The Cr(III)/Cr(VI) ratio was between 61/39 and 53/47 as determined by XPS. The chromium is distributed throughout the waste matrix and is associated with all other crystalline and amorphous phases in the waste, with slight preference to aluminum. This was determined by studying elemental maps generated by EDS.

The leaching of the chromium from the waste, was studied in two phases. First we examined the leaching properties of Cr(VI) in aqueous solutions. The release of CrO_4^{2-} from the waste material occurs when the chromium waste is immersed in pure water. The leachability of the CrO_4^{2-} has been greatly enhanced by adding salts to the water. At high pH (around 11) we found that Na_2SO_4 was the most efficient salt for removing chromate from the waste. Under optimized conditions (5 g of waste in 500 ml of 0.1 M Na_2SO_4), we were able to remove 39 % of the total chromium in the waste as chromate. However, it takes several days to reach a 39 % removal. We proposed a treatment technique where we could remove the same 39 % of total chromium in three steps in a very

short time. In the first two steps, we performed leaching with 0.1 M Na_2SO_4 salt solutions and in the third step a 0.2 M $NH_4F.HF$ salt solution was used. $NH_4F.HF$ was found to be very efficient in the removal of chromate at low pH (around 5). Furthermore, $NH_4F.HF$ seems to seal the waste and prevent further leaching of chromium into the environment (Ref. 3). After the treatment, the waste was immersed in pure water. No chromium was released from the treated waste. This demonstrates the success of our process. By modeling the kinetics of leaching chromate from waste, we were able to explain the mechanism of the leaching process. The leaching of chromate in the solution can be divided in two steps:

1. The first step where an immediate dissolution takes place _ surface chromate is readily soluble in H_2O.
2. The second step where a slow leaching takes place as part of an ion-exchange at accessible surface pores.

In a second part, we studied the leaching of Cr(III) into an aqueous solution by the process of oxidative dissolution. Depending on the pH, we could determine the following mechanisms:

1. At low pH (around 3) $Cr(OH)_3.nH_2O$ was leached from the waste by straight dissolution of Cr^{3+} followed by a oxidation to $HCrO_4^-$ in the leaching solution.
2. At higher pH (5 and higher) the Cr(III) is released from the waste by oxidative dissolution. The oxidation of $Cr(OH)_3.nH_2O$ to chromate occurs at the interface between waste particles and the leaching solution. The oxidation is then followed by dissolution of the formed chromate into the solution.

The amounts of Cr(III) that are leached out remains very low when the oxidative dissolution occurs. The maximum of Cr(III) removed under these conditions was 3.8 % of the total chromium (pH 5 with 0.08 M $KMnO_4$). Based on a kinetics experiment, we were able to determine that the leaching of Cr(III) follows a transport controlled reaction mechanism. Here, the transport controlling step is the diffusion through the complex microstructure of the waste material. The mass transport restriction is probably the main reason why the leachability of Cr(III) is low. This process is extremely important, especially with respect to cleanup standards proposed by NJ-DEP. Further research in this area is needed to define the role of Cr(III) in environmental leaching and its effect on human health.

REFERENCES

1. Cahn, R. W., Lifshin, E., 1993. *Concise Encyclopedia of Materials Characterization,* Pergamon Press, Oxford.

2. Forstner, U., Wittmann, G. T. W., 1979. *Metal Pollution in the Aquatic Environment*, Springer-Verlag, Berlin Heidelberg.

3. Labib, M. E., 1993. "Passivating Thin Film For Superconducting Material." , *United States Patent*, Patent Nr. 5,130,295.

4. Mesuere, K., Fish, W., 1992. "Chromate and Oxalate Adsorption on Goethite. 1. Calibration of Surface Complexation Models.", *Environ. Sci. Technol.*, Vol. 26, Nr. 12, p. 2357 - 2364.

5. MetCalfe, I. M., Healy, T. W., 1990. " Charge-regulation Modeling of the Schultze-Hardy Rule and Related Coagulation Effects.", *Faraday Discuss. Chem. Soc.*, Vol. 90, p. 335 - 344.

6. Nriagu, J. O., Nieboer, E., 1988. *Chromium in the Natural and Human Environments*, John Wiley & Sons, New York, NY.

7. Ososkov, V., Bozzelli, J. W., 1994. " Removal of Cr(VI) from Chromium Contaminated Sites by Washing with Hot Water.", *Hazardous Waste & Hazardous Materials*, Vol. 11, Nr. 4, p. 511-517.

8. Pourbaix, M., 1966. *Atlas of Electrochemical Equilibria in Aqueous Solutions*, Pergamon Press, Oxford.

9. Public Health Service, 1953. *The Chromate-producing Industry. In: Health of Workers in Chromate Producing Industry - A Study.* Federal Security Agency, Public Health Service, Publication Nr. 192.

10. Reartes, G. B., Morando, P. J., Blesa, M. A., Hewlett, P. B., Matijevic, E., 1991. " Reactivity of Chromium Oxide in Aqueous Solutions. 1. Oxidative Dissolution.", *Chem. Mater.*, Vol. 3, p. 1101 - 1106.

11. Stumm, W., 1992. *Chemistry of the Solid - Water Interface*, John Wiley & Sons, New York, NY.

12. Weng, C. H., Huang, C. P., Allen, H. E., Cheng, A. H-D., Sanders, P. F., 1994. " Chromium Leaching Behavior in Soil Derived from Chromite Ore Processing Waste.", *The Science of the Total Environment*, Vol. 154, p. 71 - 86.